

Atomtronic circuits: from basic research in many-body physics to applications for quantum technologies*

Luigi Amico

Quantum Research Centre, Technology Innovation Institute, Abu Dhabi, UAE[†]

INFN-Sezione di Catania, Via S. Sofia 64, 95127 Catania, Italy

Centre for Quantum Technologies, National University of Singapore, 3 Science Drive 2, Singapore 117543, Singapore and

LANEF 'Chaire d'excellence', Université Grenoble-Alpes & CNRS, F-38000 Grenoble, France

Dana Anderson

Department of Physics and JILA, University of Colorado, Boulder, Colorado, 80309-0440, USA

Malcolm Boshier

MPA Division, Los Alamos National Laboratory, Los Alamos, NM 87545, USA

Jean-Philippe Brantut

Institute of Physics, EPFL, 1015 Lausanne, Switzerland

Leong-Chuan Kwek

Centre for Quantum Technologies, National University of Singapore, 3 Science Drive 2, Singapore 117543, Singapore

MajuLab, CNRS-UNS-NUS-NTU International Joint Research Unit, UMI 3654, Singapore and

Institute of Advanced Studies, Nanyang Technological University, 60 Nanyang View, Singapore 639673, Singapore

Anna Minguzzi

Université Grenoble-Alpes and CNRS, LPMMC, F-38000 Grenoble

Wolf von Klitzing

Institute of Electronic Structure and Laser, Foundation for Research and Technology—Hellas, Heraklion 70013, Greece

Atomtronics is an emerging field which aims to manipulate ultracold atom moving in matter wave circuits for both fundamental studies in quantum science and technological applications. In this colloquium, we review recent progress in matter-wave circuitry and atomtronics-based quantum technology. After a short introduction to the basic physical principles and the key experimental techniques needed to realize atomtronic systems, we describe the physics of matter-wave in simple circuits such as ring traps and two-terminal systems. The main experimental observations and outstanding questions are discussed. Applications to a broad range of quantum technologies, from quantum sensing with atom interferometry to future quantum simulation and quantum computation architectures, are then presented.

Contents

I. Introduction	2	1. Magnetic traps	4
II. Traps and Guides	2	2. Atom Chip Technology: Trapping atoms above the surface	5
A. Optical Potentials	2	3. Adiabatic Magnetic Potentials	6
1. Waveguides and traps formed with static laser beams	3	4. Time-Averaged Adiabatic Potentials (TAAPs)	7
2. Time-averaged optical potentials	3	C. Atom optical elements	8
3. Spatial light modulators	4	1. Waveguides	8
4. Other approaches	4	2. Ring traps	8
B. Magnetic potentials	4	3. Barriers and beam splitters	9
III. Coherent effects in mesoscopic matter-wave circuits	9		
A. Model Hamiltonians	10		
1. Bosons	10		
2. Fermions	11		
3. Impurities, weak-links and contacts	12		
B. Persistent currents in atomtronic circuits	12		
1. The concept of persistent current	12		
2. Experimental observation in ultracold atom setups	14		

*This article is dedicated to the memory of Frank Hekking.

[†]On leave from Dipartimento di Fisica e Astronomia, Via S. Sofia 64, 95127 Catania, Italy

3. Readout of the current state	14
4. Persistent current in fermionic rings	14
C. Two terminal quantum transport in cold atom mesoscopic structures	15
1. Double well systems	15
2. Conductance measurements and incoherent reservoirs	17
3. Two terminal transport through ring condensates	19
IV. Atomtronic Components and Applications	20
A. Matter wave optics in atomtronic circuits	20
B. Transistors, diodes, and batteries	20
C. Atomtronic qubit implementations	21
D. Atomtronic Interferometers	23
V. Remarks and Future Perspectives	24
Acknowledgments	25
References	25

I. INTRODUCTION

Atomtronics is the emerging quantum technology of ultra-cold atoms moving in matter-wave circuits (Amico *et al.*, 2017, 2020, 2005; Seaman *et al.*, 2007). For the implementations realized to date, matter waves travel in guides made of laser light or magnetic fields. These approaches offer highly controllable, flexible and versatile platforms at the microscopic spatial scale (Gauthier *et al.*, 2019; Henderson *et al.*, 2009; Rubinsztein-Dunlop *et al.*, 2016). Foundational works for integrated atom optics circuits are (Denschlag *et al.*, 1999a,b; Schmiedmayer, 1995b; Schmiedmayer and Scrinzi, 1996a,b). The quantum fluid flowing through the circuits is provided by ultracold atoms that can be fermions, bosons, or a mixture of the two species. Cold atom quantum technology allows coherent matter-wave manipulations with unprecedented control and precision over a wide range of spatial lengths and physical conditions (Bloch, 2005; Cornell and Wieman, 2002; Dalfovo *et al.*, 1999; Ketterle, 2002).

Atomtronic circuits are therefore suitable as cold-atom quantum simulators (Bloch, 2005; Buluta and Nori, 2009; Cirac and Zoller, 2012; Dowling and Milburn, 2003; Lamata *et al.*, 2014; Lewenstein *et al.*, 2012) in which matter wave currents can be harnessed as probes to explore the physics of the system. In this way, important problems in fundamental quantum science, such as superfluidity, strong correlations in extended systems, topological aspects in quantum matter, quantum transport, and various mesoscopic effects, can be addressed in new physical regimes and configurations. (Burchianti *et al.*, 2018; Del Pace *et al.*, 2021; Husmann *et al.*, 2015; Krinner *et al.*, 2016; Stadler *et al.*, 2012; Valtolina *et al.*, 2015).

At the same time, atomtronic circuits can play an important role in applied science and technology. Like electronic devices, atomtronic circuits operate over a separation of time and length scales between devices and leads. This permits the construction of standardized functional units connected to each other by wires or waveguides.

Atomtronic counterparts of known electronic or quantum electronic components have been the first developments in the field. Some examples include atomtronic amplifiers, diodes, switches, batteries, memories (Anderson, 2021; Caliga *et al.*, 2017, 2016b; Pepino *et al.*, 2009; Pepino, 2021; Seaman *et al.*, 2007; Stickney *et al.*, 2007; Zozulya and Anderson, 2013). Moreover, cold atom realizations of Josephson junctions have led to the fabrication and analysis of atomtronic superconducting quantum interference devices (SQUIDs) (Aghamalyan *et al.*, 2015; Amico *et al.*, 2014; Eckel *et al.*, 2014b; Haug *et al.*, 2018b; Jendrzejewski *et al.*, 2014; Ramanathan *et al.*, 2011; Ryu *et al.*, 2013, 2020; Wright *et al.*, 2013a). Atomtronics can contribute to the field of quantum sensors (Bongs *et al.*, 2019; Cronin *et al.*, 2009; Degen *et al.*, 2017). In particular, several solutions for compact interferometers with enhanced sensitivity to inertial forces, gravity, and electromagnetic fields have been studied (Akatsuka *et al.*, 2017; Burke and Sackett, 2009; Kim *et al.*, 2021; Krzyzanowska *et al.*, 2021; Moan *et al.*, 2020; Qi *et al.*, 2017; Ryu and Boshier, 2015; Wang *et al.*, 2005; Wildermuth *et al.*, 2006; Wu *et al.*, 2007).

We finally note that highly sophisticated devices and functionalities that have no analogue in electronics or in photonics can be built from microscopic descriptions with the aforementioned enhanced control (Bloch *et al.*, 2008; Lewenstein *et al.*, 2012) - see (Amico *et al.*, 2017) for a recent survey.

This Colloquium is organized as follows: In Sec. II, we discuss the state of the art of the optical trapping technology that leads to a variety of circuits. In Sec. III, we focus on the coherent flow in simple atomtronic networks of mesoscopic size. In this section, we bridge many-body models with persistent currents and two-terminal transport through a mesoscopic channel. In Sec. IV we describe some of the components that have been studied and developed so far. Finally, we conclude and provide some outlooks in Sec. V.

II. TRAPS AND GUIDES

Cold atoms can be trapped in controllable and flexible potentials. These potentials are produced either by optical fields that exert forces on atoms through their polarizability or by magnetic fields that create forces on atomic magnetic dipoles. Both approaches offer an avenue to realize complex potentials in which matter waves are created, guided, and manipulated.

A. Optical Potentials

The formation of optical potentials through static or dynamic laser beams is a mature technology for the realization of atomtronic circuitry. The flexible potentials can have almost arbitrary complexity in both spatial and time domains.

Optical manipulation of ultracold atoms is based on the electric dipole interaction between the atoms and the laser beam. When the laser frequency ω is far-detuned from an atomic transition of frequency ω_0 , the interaction energy takes the form of an optical dipole potential

$$U(\mathbf{r}) = -\frac{3\pi c^2}{2\omega_0^3} \frac{\Gamma}{\Delta} I(\mathbf{r}). \quad (1)$$

where $\Delta = \omega - \omega_0$ is the detuning, Γ is the natural decay rate of the population of the excited state, and $I(\mathbf{r})$ is the position-dependent laser intensity. This dipole force can be attractive ($\Delta < 0$ or “red-detuned”) or repulsive ($\Delta > 0$ or “blue-detuned”) (Grimm *et al.*, 2000). The detuning should be large enough so that spontaneous scattering is negligible on the timescale of the experiment.

1. Waveguides and traps formed with static laser beams

Waveguides supporting coherent propagation of matter waves must be smooth to avoid excitations out the guide ground state to higher modes, and stable because fluctuations in the potential cause fluctuations in the phase accumulated by the matter wave. A collimated laser beam is a straightforward solution to this problem. The first guides for cold, non-condensed atoms used the evanescent field of blue-detuned light propagating in a hollow optical waveguide (Müller *et al.*, 2000; Renn *et al.*, 1996; Rhodes *et al.*, 2002). This was followed by the introduction of traps and guides based on hollow blue-detuned laser beams created with doughnut or Laguerre-Gaussian transverse modes that removed the need for a material optical guide (Kuga *et al.*, 1997). This approach enabled creation of the first waveguide for a Bose-Einstein condensate (BEC) (Bongs *et al.*, 2001). When the Laguerre-Gaussian beam is tightly focused, the optical dipole potential becomes more like a toroidal trap (Olson *et al.*, 2007) than a waveguide. Waveguide potentials can also be realized with Bessel beams (Arlt *et al.*, 2000).

Red-detuned collimated laser beam is a simpler technology for creating atomtronic waveguides when spontaneous emission is sufficiently small. An early example of this approach was the realization of a simple beamsplitter for propagating cold thermal atoms with a pair of crossed red-detuned laser beams (Houde *et al.*, 2000). Subsequent demonstrations include coherent propagation of BEC matter wavepackets to realize a Mach-Zehnder atom interferometer (Kim *et al.*, 2021; McDonald *et al.*, 2013a), a beamsplitter for BECs (Gattobigio *et al.*, 2012) and a waveguide Sagnac atom interferometer (Krzyszowska *et al.*, 2021). Red-detuned collimated lasers are also used to guide the matter wave produced by an atom laser (Couvert *et al.*, 2008; Dall *et al.*, 2010; Guerin *et al.*, 2006). A very recent development is the use of clipped gaussian beams to create elongated trapping and guiding potentials (Lim *et al.*, 2021).

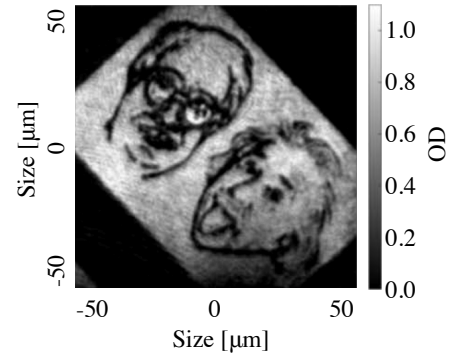


FIG. 1 A Bose-Einstein condensate created in a potential made by imaging a sketch of Bose and Einstein with a digital micro-mirror device (DMD) (Gauthier *et al.*, 2016)

2. Time-averaged optical potentials

Optical dipole potentials based on static laser beams are cylindrically symmetric and they can have no time dependence beyond a scaling of the trap strength. This shortcoming motivated the development of time-averaged optical potentials. Similar to the guides discussed above, the initial experiments with this approach used non-condensed thermal atoms, confining them to box and stadium potentials with walls formed by a blue-detuned laser beams that was rapidly scanned with a pair of acousto-optic deflectors (Friedman *et al.*, 2001; Milner *et al.*, 2001). While early experiments on trapping Bose-Einstein condensates (BECs) in multiple wells formed by rapidly switching the position of a single red-detuned laser found that the condensates were heated (Onofrio *et al.*, 2000), that issue was absent in later work in which a time-averaged tightly-focused laser beam “painted” a desired potential on a canvas provided by a light sheet that confined atoms to a horizontal plane. This “painted potential” (Henderson *et al.*, 2009; Schnelle *et al.*, 2008) is able to realize arbitrary and dynamic 2D matter waveguide structures. This includes the important case of toroidal potentials, (Bell *et al.*, 2016; Henderson *et al.*, 2009; Ryu *et al.*, 2014), where periodically reducing the intensity the laser painting the attractive potential creates movable repulsive barriers that can form Josephson junctions in an atom SQUID geometry (Ryu *et al.*, 2013, 2020). Repulsive barriers can also be imposed on a trap by painting with a blue-detuned laser (Ramanathan *et al.*, 2011; Wright *et al.*, 2013a). A significant advantage of this approach is that a suitable modulation of the tweezer beam intensity as it paints the atomtronic circuit can flatten out any imperfections in the potential (Bell *et al.*, 2016; Ryu and Boshier, 2015), enabling creation of waveguides smooth enough to support single mode propagation and to realize the first coherent beam splitter for propagating matter waves (Ryu and Boshier, 2015).

While painting has the advantages of making efficient use of laser power and enabling fine control of the shape of the potential landscape, it has some limitations. The

time averaging requirement that the potential be painted at a rate significantly higher than the guide trapping frequency limits the trapping frequencies attainable with current acousto-optic deflector technology to several kHz. While it is usually a good approximation to regard the painted potential as static, in some circumstances the time-varying phase imprinted by the painting beam can be an issue (Bell *et al.*, 2018).

3. Spatial light modulators

A second technology for creating complex 2D potential landscapes on a light sheet relies on spatial light modulators (SLMs) that can impose amplitude or phase modulation on a laser beam which forms the desired potential after propagation through suitable optics. Two approaches have been demonstrated: a Fourier optics approach in which the SLM acts as a hologram, and a direct imaging of an intensity pattern formed by the SLM. A detailed discussion of the production of arbitrary optical potentials is presented in reference (Gauthier *et al.*, 2021).

Early work in this direction used liquid crystal modulators to create phase holograms producing arrays of tweezer beams (Curtis *et al.*, 2002) or more complex geometries (Boyer *et al.*, 2004, 2006; Gaunt and Hadzibabic, 2012). Liquid crystal SLMs are now widely used in creating dynamic optical tweezer systems for assembling arrays of Rydberg atoms used for quantum information processing (Nogrette *et al.*, 2014). Advantages of liquid crystal modulators include the ability to impose phase or amplitude modulation on an optical beam and the possibility of using them either as holographic elements or for direct imaging, as well as a high power efficiency. The disadvantages include a limited response time for creating time-dependent potentials, as well as the technical overhead of computing real-time SLM holograms for dynamic potentials, which can be addressed using increasingly powerful GPUs.

An alternative to SLMs are digital micromirror devices (DMDs), producing binary patterns over a matrix of individually switched mirrors. The intensity pattern formed by the DMD can be imaged directly onto an atomic cloud using standard imaging, to form intricate potentials in the image of the optical system. Fine intensity control overcoming the binary nature of the DMD can then be achieved through half-toning techniques (Gauthier *et al.*, 2021, 2016; Kumar *et al.*, 2016a; Tajik *et al.*, 2019; Zou *et al.*, 2021). DMDs can also be used as programmable diffraction gratings, similar to SLMs, at the expenses of low power efficiency (Zupancic *et al.*, 2016). They offer however higher refresh rate, allowing for their use in dynamical experiments (Ha *et al.*, 2015). Fig. 1 illustrates the power of this technique for creating a BEC in the shape of a sketch of Bose and Einstein. DMDs do suffer from flickering modulation due to their intended use in image projectors for the consumer market and so

some devices may require customization for optimal use (Hueck *et al.*, 2017).

4. Other approaches

Other, more specialized approaches, to creating optical potentials include the use of arrays of micro-lenses realize geometries analogous to an array of Mach-Zehnder interferometers (Dumke *et al.*, 2002) and the application of conical refraction in a biaxial crystal to realize a large ring waveguide (Turpin *et al.*, 2015) that could be used as the basis of an atom interferometer.

Standing waves of laser light form periodic potentials that are used in atomtronic circuitry. For example, standing waves impressed on a collimated laser waveguide have been shown to form a distributed Bragg reflector (Fabre *et al.*, 2011). Pulsed optical standing waves are also employed as beam splitters in waveguide atom interferometers (Kim *et al.*, 2021; Krzyzanowska *et al.*, 2021; Wang *et al.*, 2005; Wu *et al.*, 2005).

B. Magnetic potentials

1. Magnetic traps

Magnetic trapping lies at the heart of many cold atoms quantum technologies. Here, we sketch the logic of the technique. Magnetic traps confine spin-polarized atoms of non-zero magnetic moment to a local minimum of an external magnetic field \mathbf{B} . If the magnetic field at the center of mass position of an atom is sufficiently large and varies slowly, then its spin follows its change in direction and magnitude. The Zeeman energy of spin polarized atoms ($V = -\mu \cdot \mathbf{B}$) can then be written as $V = m_F g_F \mu_B |\mathbf{B}|$, with $m_F = \{-F \dots F\}$ being the magnetic hyperfine number, g_F the Landé g -factor, and μ_B the Bohr magneton. Unfortunately, Maxwell's equations forbid the generation of a dc-magnetic field maximum in free space. Therefore, one has to trap so-called low-field seeking states, whose energy increases with magnetic field strength. The field strength of the magnetic minimum has to be sufficiently large in order to prevent non adiabatic spin-flip transitions to lower-energy (high-field seeking) states. The latter can cause atoms to be expelled from the trap (Majorana, 1932). The two most common magnetic configurations are the Ioffe-Pritchard (IP) (Baiborodov *et al.*, 1963; Pritchard, 1983) and the time-orbiting potential (TOP) (Petrich *et al.*, 1995) traps.

An IP trap consists of a radial quadrupole and an axial parabolic field for a very elongated trap is:

$$\mathbf{B}_{\text{IP}} = \alpha (x \hat{\mathbf{e}}_x - y \hat{\mathbf{e}}_y) + \left(B_0 + \frac{1}{2} \beta z^2 \right) \hat{\mathbf{e}}_z \quad (2)$$

where α is the radial gradient, β the curvature of the trap, B_0 the offset field in the center of the trap and $\hat{\mathbf{e}}_x$,

\hat{e}_y , and \hat{e}_z are the normal vectors of the coordinate system. The strength of the confinement is described by the radial and axial trapping frequencies, which are $\omega_\rho = (m_F g_F \mu_B m^{-1} \alpha^2 / B_0)^{1/2}$ and $\omega_z = (m_F g_F \mu_B m^{-1} \beta)^{1/2}$ respectively, with μ_B being the Bohr magneton, g_F the gyro-magnetic factor, and m the mass of a trapped atom. Typical values for the radial trap frequency range from few hundreds to few thousands Hz for chip-based traps (Hänsel *et al.*, 2001). Typical axial frequencies are a few tens of hertz. Macroscopic IP traps are usually formed from a combination of large race-track shaped coils for the radial gradient and small ‘pinch’ coils for the parabolic axial field. It is also possible to use structures from permanently magnetized materials, allowing the creation of larger magnetic gradients and thus steeper traps. They also provide a larger degree of freedom in design when compared to their purely electro-magnetic counterparts albeit at the cost of an inability to dynamically change the strength of the confinement or easily release the atoms from the trap (Davis, 1999; Fernholz *et al.*, 2008; Sinclair *et al.*, 2005; Tollett *et al.*, 1995). Another option is to locally modify an external oscillating field using inductively coupled structures (Pritchard *et al.*, 2012; Sinuco-León *et al.*, 2014).

An alternative to creating a permanent magnetic offset is to move a 3D quadrupole field of gradient α using a homogeneous offset field of amplitude B_0 , the direction of which rotates with an angular frequency ω_{mod} around the z -axis: $\mathbf{B}_{\text{TOP}} = \mathbf{B}_Q + \mathbf{B}_{\text{mod}}$ with the quadrupole field $\mathbf{B}_Q = \alpha(x\hat{e}_x + y\hat{e}_y - 2z\hat{e}_z)$ and the modulation field $\mathbf{B}_{\text{mod}} = B_0[(\sin \omega_{\text{mod}} t)\hat{e}_x + (\cos \omega_{\text{mod}} t)\hat{e}_y]$. If the modulation frequency ω_{mod} is large compared to the eventual trapping frequency and small compared to the Larmor frequency ω_L , then the radial and axial trapping frequencies are $\omega_\rho = \alpha \sqrt{m_F g_F \mu_B / (m B_0)}$ and $\omega_z = \sqrt{8} \omega_\rho$, respectively. The Larmor frequency is $\omega_L = |g_F| \mu_B |\mathbf{B}| / \hbar$.

It was soon realized that the radial confinement could also be achieved using a single wire with a transverse homogeneous magnetic field (Schmiedmayer, 1995a). This has led to the development of ‘atom chip’ traps (Folman *et al.*, 2000; Hänsel *et al.*, 2001; Reichel *et al.*, 1999) consisting of micro-sized current-carrying wires manufactured using standard semiconductor technologies. Such thin wires can be cooled very efficiently through the substrate and thus permit very large current densities resulting in very large magnetic gradients. Consequently, very high trapping frequencies, of up to 10 kHz, can be achieved. Another advantage is the ability to create easily complex 2D wire structures. For example, a magnetic IP trap can be formed with an elongated Z-shaped structure, with the vertical line producing the radial quadrupole and the two horizontal wires producing the required parabolic axial confinement. Similarly, a 3D quadrupole trap can be created using a simple U-shaped wire (Reichel *et al.*, 1999) and a 2D-quadrupole can be formed from three parallel wires, thus creating a matter wave waveguide along which atoms are propagated (Folman *et al.*, 2000; Long *et al.*, 2005).

2. Atom Chip Technology: Trapping atoms above the surface

In macroscopic traps, the maximum power and current density limit the maximal confinement that can be achieved. Furthermore, the distance of the coils limits the complexity of the potentials that can be created. Atom chips use very small wires on a solid substrates (typically silicon and glass), thus enabling extremely large current densities (and thus magnetic gradients α) and more complex geometries. (Folman *et al.*, 2000; Fortágh and Zimmermann, 2007; Keil *et al.*, 2016). Simple H-, T-, U-, Y- and Z-shaped wires can create a wide range of fields such as the ones required for Ioffe-Pritchard (IP) or magneto-optical traps (MOT) (Reichel *et al.*, 1999). Atom chips cooled to cryogenic temperatures have also allowed superconducting devices to be incorporated (Mukai *et al.*, 2007; Nirrengarten *et al.*, 2006; Salim *et al.*, 2013). Atom chips have thus become compact hybrid platforms to trap, prepare, manipulate, and measure cold atoms. They provide the route for miniaturization and interfacing different atomtronic components in more complex devices (Birkl *et al.*, 2001; Gehr *et al.*, 2010; Salim *et al.*, 2013).

Aside from neutral atoms, chip technology can be extended to the trapping and manipulation of Rydberg atoms (Naber *et al.*, 2016; Saffman *et al.*, 2010), fermions (Aubin *et al.*, 2006; Truscott *et al.*, 2001), molecules (Meek *et al.*, 2008, 2009; Rieger *et al.*, 2005; Shuman *et al.*, 2010), and charged particles (Folman *et al.*, 2000).

a. Noise in Atom-Chip Potentials The resolution for the tailored fields is typically of the order of the distance from the field source. So the construction of the atomic circuit at a distance of no more than a few micro-meters from the surface of the chip is required. At this tiny scales, atom chips need to surmount some inherent challenges. Bringing atoms closer to the chip surface inevitably leads to stray fields and other disruptive noises. These noises can emerge from diverse causes, like for instance current scattering due to unintended changes in flow of direction of the current, noises in the power supplies, or magnetic impurities (Kraft *et al.*, 2002; Krüger *et al.*, 2007; Leanhardt *et al.*, 2002). Such technical noises constitute the strongest source of noise in most atom chips. The consequent atomic density variation results in the fragmentation of the atom cloud into several separated components as it is brought close to the surface (David *et al.*, 2008).

The other type of noise is Johnson noise, whose origin stems from thermal energy. As the atoms approach the surface, these noises increase. Johnson noise could be mitigated with lower conductance materials (Dikovsky *et al.*, 2005), thinner layers or alloys. Surprisingly, it has been shown that superconducting surfaces possess low level of noises (Dikovsky *et al.*, 2009; Kasch *et al.*, 2010; Müller *et al.*, 2010a,b). Decoherence phenomena arising from these noises pose significant problems for the preservation of coherence of the atoms as well as the trapping

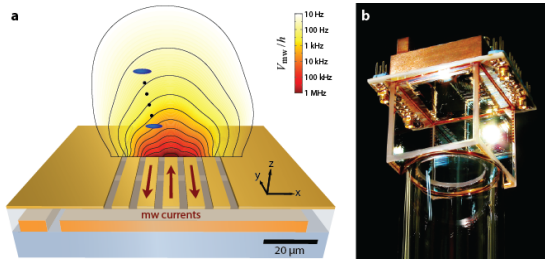


FIG. 2 Atom chip used for double well physics in 1D and crossover regimes, which is enabled by the ability to create robust double-well potentials using rf dressing of the atoms. Fast trap modulations are used in optimal control schemes, allowing one to engineer the external state of the condensates, which was used, for instance, for the highly efficient creation of twin-atom beams. Furthermore, a unique time-of-flight fluorescence imaging system allows one to work with extremely dilute clouds and provides single atom sensitivity, which promotes experiment in quantum matter-wave optics, such as Hanbury Brown-Twiss type measurements of second-order correlations in expanding clouds.

and manipulation of the atoms. However, with continued improvement in chip fabrication techniques, advancement in multi-layer structures and thin film magnetic materials (Folman *et al.*, 2008), one should be able to overcome some of the noises and limitations in current designs.

Another type of noise related to the propagation along a waveguide on the chip occurs when there is any corrugation of the waveguide potential. The corrugation couples the forward motion to the transverse vibrationally excited modes causing heating and loss of contrast in atom interferometry. It appears that these corrugations are almost unavoidable in magnetic fields due to the meandering nature of the flow of electrons even if the conductor itself is perfectly smooth. The corrugation of the magnetic potential drops off exponentially with distance according to $\exp(-k\rho)/\sqrt{k\rho}$, where ρ is the distance from the conductor and $k = 2\pi/\lambda$ is the characteristic spatial frequency of corrugations of length scale λ (Jones *et al.*, 2004). One can therefore move further away from the wire, in order to reduce the deleterious effects of the corrugations, albeit at the cost of reduced magnetic gradient α and thus confinement. One can also reduce the corrugations by modulating the current in the wires (Trebbia *et al.*, 2007) or using adiabatic potentials (Schumm *et al.*, 2005). However, the mere fact that the shape of the atom chip potentials is defined by wire structures means that any imperfections in the wires cause defects and roughness in these potentials and make the single mode propagation very difficult.

b. Ultracold atom-superconductor hybrid networks Superconducting devices are increasingly relevant for quantum technology. Here we review some recent progresses of ultracold atoms coupled with superconducting solid state

devices hybrid systems.

The atomic spins are indeed very sensitive to microwaves (Fleischhauer *et al.*, 2005; Hammerer *et al.*, 2010). Therefore coupled systems of atoms and superconducting elements have been proposed with an objective of defining hybrid devices. For instance, in a schematic information processing protocol, the operations for (entangled) state preparation are carried out in the fast solid state gates; the states are then transferred and stored in atomic systems which have longer decoherence times before eventually transferring back to solid state devices for further processing. Such logic has been studied in a number of theoretical proposals and implementations (Xiang *et al.*, 2013; Yu *et al.*, 2017a,b, 2018a,b, 2016a,b,c).

The fabrication and characterization of various magnetic traps for ultracold atoms on superconducting atom chips have also been successfully demonstrated (Cano *et al.*, 2008; Mukai *et al.*, 2007; Müller *et al.*, 2010a,b; Nirrengarten *et al.*, 2006; Tosto *et al.*, 2019; Zhang *et al.*, 2012). These experiments have demonstrated that it is possible to suppress noise sufficiently and attain enhanced coherence.

The coupling between ultracold atoms and superconducting chips for quantum information processing has also been studied in (Bertron *et al.*, 2013; Fortágh and Zimmermann, 2007; Hattermann *et al.*, 2017; Petrosyan *et al.*, 2019; Verdú *et al.*, 2009). Such system paves the way towards the realization of an atomic quantum memory coupled to superconducting quantum circuits.

3. Adiabatic Magnetic Potentials

Adiabatic magnetic potential offer a very interesting alternative to chip-based structure in that it can be used to create a limited number of perfectly smooth trapping structures such as bubbles, rings and sheets. It is based on the dressed dressed-atom picture (Cohen-Tannoudji and Reynaud, 1977) with a radio-frequency field (\mathbf{B}_{rf}) strongly coupling magnetic hyperfine states. When the radio frequency field is resonant with the magnetic field, i.e. $\omega_{\text{rf}} = \omega_L$, then the coupling strength can be expressed as the Rabi frequency $\Omega_0 = g_F \mu_B B_{\text{rf}}^{\perp} / \hbar$, where B_{rf}^{\perp} is the amplitude of the circularly polarized component of \mathbf{B}_{rf} that is orthogonal to \mathbf{B} and couples the m_F states. For an arbitrary detuning ($\delta = \omega_{\text{rf}} - \omega_L$) of the rf-field from the resonance the dressed potential can be expressed as $U(\mathbf{r}) = m'_F \hbar \sqrt{\delta^2(\mathbf{r}) + \Omega_0^2(\mathbf{r})}$. Note that the potential is equal to the non-dressed Zeeman states with $m'_F = m_F$ for $\delta \gg \Omega_0$, and inversely that it is equal to the non-dressed Zeeman states with $m'_F = -m_F$ for $\delta \ll -\Omega_0$. A sketch of the dressing can be seen in Fig. 3.

Let us examine the simple case of a magnetic quadrupole field, where the magnitude of the field increases linearly in all directions. In any direction starting from the center outwards, there is some point at which the rf field becomes resonant. The dressed field therefore forms an oblate bubble shaped trap, which has a

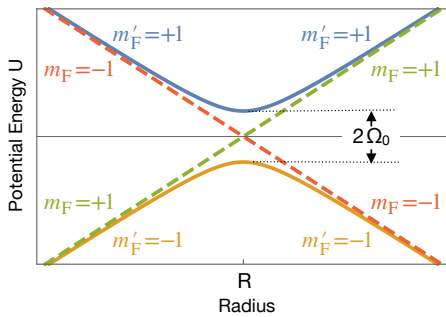


FIG. 3 Adiabatic potentials (solid lines) with their corresponding unperturbed Zeeman states (dashed). The two adiabatic potentials are split by twice the Rabi frequency: $U = 2\hbar\Omega_0$.

radius of $r_\rho = \hbar\omega_{\text{rf}} / (|g_F| \mu_B \alpha)$ in the x/y plane and $r_z = \hbar\omega_{\text{rf}} / (|g_F| \mu_B 2\alpha)$ in the z-direction. The original idea was proposed in (Zobay and Garraway, 2001) and first realised in (Colombe *et al.*, 2004). A thorough review of these traps is found in (Garraway and Perrin, 2016; Perrin and Garraway, 2017). Nevertheless, the dressed quadrupole field itself presents a problem: any homogeneous B_{rf} has one or two points on the bubble, where due to the projection of the rf onto the local quadrupole field the coupling field B_{rf}^\perp is zero, leading to Majorana spin-flip losses. This can be avoided using a IP-type trap, where the magnetic field points predominantly in the direction of the z-axis. In the absence of gravity, the quantum fluid can fill the entire bubble (Sun *et al.*, 2018). These hollow Bose-Einstein condensates are currently under investigation at the international space station (Frye *et al.*, 2021). On earth however, gravity deforms the bubble-trap into something more akin to a cup, which can be exploited for 2D quantum gasses for its strong (weak) confinement in the vertical (horizontal) direction. Using multiple rf-frequencies, multiple shells can be manipulated almost independently (Bentine *et al.*, 2017) and exploited for matter wave interferometry (Mas *et al.*, 2019). Recently, an interesting method has emerged to create non-trivial geometries, i.e. a matter wave ring, by applying angular momentum to the trapped atoms and thus approaching a giant vortex state (Guo *et al.*, 2020). Alternatively, one can combine the rf-bubble trap with a red-detuned light-sheet, thus forming a ring-shaped trap (Morizot *et al.*, 2006).

4. Time-Averaged Adiabatic Potentials (TAAPs)

Highly versatile and controllable potentials in a great variety of shapes can be created by combining the aforementioned adiabatic potentials of the bubble trap with an oscillating, homogeneous magnetic field. If the Rabi frequency of the rf dressing field is large compared to the frequency of the oscillating field $\Omega_0 \gg \omega_m$, the resulting trapping potential is the time-average of the adiabatic

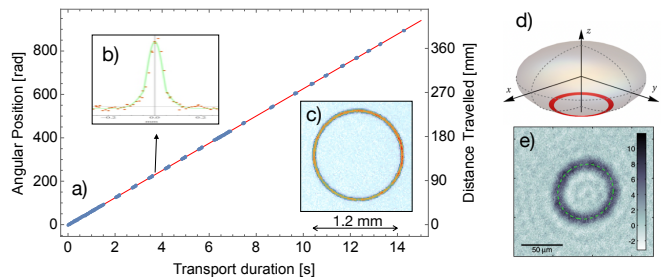


FIG. 4 a) Long distance transport in a ring-shaped TAAP wave-guide. The plot shows the angular position of the condensate and thermal cloud during 14s of transport in the matter-wave guide (blue dots) over a distance of more than 40cm. The red line depicts the programmed trajectory of $2\pi 10 \text{ rad s}^{-1}$. b) The bi-modal distribution of the BEC after 4.1s of transport and a time of flight expansion of 24ms, with the black arrow indicating to the relevant data point (Pandey *et al.*, 2019). c) A false-color absorption image of an annular condensate in a TAAP trap. d) A graphical illustration of atoms in a dynamically created ring trap (Guo *et al.*, 2020) and e) an absorption image of a BEC in it.

and modulation potentials (Lesanovsky and von Klitzing, 2007; Navez *et al.*, 2016). Starting with a simple quadrupole field and adding a vertically polarized rf-field, plus a vertical modulation field, one can generate a ring-shaped trap, resulting in the trapping potential of the form

$$V_r(r, z) = \hbar\Omega_0 + \frac{1}{2}m\omega_r^2(r - R)^2 + \frac{1}{2}m\omega_z^2z^2 - \frac{\delta}{2}mgR \cos(\phi - \phi_0), \quad (3)$$

where R is the radius of the ring, ω_r and ω_z are the radial and the axial trapping frequency, respectively. Typical values are 50 Hz to 100 Hz for the trapping frequencies and 50 μm to 1 mm for the radius. The ring can then be adiabatically turned into one or two coupled half-moon shaped traps simply by changing the polarization of the rf or modulation fields. Multiple concentric or stacked rings can be created by using more than one rf-frequency.

The exact shapes of these traps and the barriers between them depend only on the amplitude and polarization of oscillating magnetic fields, which can be adjusted with extreme precision using standard electronics; making it possible to control the trapping potentials down to the picokelvin level.

Using a suitable choice of polarizations, it is also possible to trap two different spin states in identical effective potentials and even to manipulate them entirely independently (Navez *et al.*, 2016). This technique might be exploited in an atom interferometer, where the atoms are placed in the TAAP in a single hyperfine state and exposed to a suitable microwave pulse. The hyperfine states of the resulting superposition can then be manipulated separately, making them sensitive to gravitation, for instance, and then recombining with a second microwave pulse - resulting in a highly sensitive interfer-

ometer (Navez *et al.*, 2016). A similar scheme has been proposed for adiabatic ring-shaped potentials resulting from specially tailored magnetic fields (Stevenson *et al.*, 2015).

Another feature of the TAAP rings is the extreme smoothness of these potentials (Pandey *et al.*, 2019). Its shape is not determined by current carrying structures in proximity but by a quadrupole field and the frequency and amplitude of modulations fields, which are all generated by very distant coils. Therefore, any imperfections in the field-generating coils are exponentially suppressed on the size-scale of the trapping potentials. This was evidenced in Ref. (Navez *et al.*, 2016), where a Bose-Einstein condensate was transported at hypersonic speeds for a distance of 15 cm without loss in spatial coherence.

C. Atom optical elements

In this section we outline the types of potentials and the optical elements that have been designed to guide the matter-wave in atomtronic circuits.

1. Waveguides

The fabrication of one dimensional guides is important in the atomtronics context, both to control the circuit functionalities and to explore quantum effects in fundamental physics. The coherent regime needs to consider both the tightness of the confinement and any displacement of the waveguide transverse to the direction of propagation. Operating in the strict one-dimensional regime requires the transverse frequencies to be much larger than both the chemical potential and the temperature of the gas, as well as the kinetic energy originating from the current flowing in the system. This can be achieved using tight optical confinement from optical lattices (Bloch *et al.*, 2008) or projected wires (Krinner *et al.*, 2017). Optical lattices with a typical lattice spacing of few microns have been realized (Rubinsztein-Dunlop *et al.*, 2016). In such structures, in which the cold atoms can tunnel between the lowest Bloch bands of the adjacent wells, the low temperatures matter-wave effective dynamics is one dimensional.

A modulation of the strength of the transverse confinement or a bend in the waveguide couples the forward motion of the atoms to oscillations of the condensate via its chemical potential. It also causes a shift of the potential energy of the bottom of the waveguide, which can induce scattering. As pointed out in section II.B.2.a, this regime is very difficult to achieve with atom chips. Excitationless matter-wave guides have been demonstrated using single-beam optical dipole beams over distances of 3.5 mm (McDonald *et al.*, 2013a) and using TAAPs over distances of 40 cm for thermal clouds and 15 cm for BECs (Pandey *et al.*, 2019). Waveguide bends and junctions

created with painted potentials have demonstrated excitation probabilities of less than 8% (Ryu and Boshier, 2015).

The requirements for precision interferometers are rather stringent. Great care must be taken that the superposition state traverses the interferometer adiabatically and that the trap-induced energy difference between the two paths is extremely well controlled (Kreutzmann *et al.*, 2004; Zabow *et al.*, 2004). For the propagating matter wave interferometers this results in extreme requirements on corrugations of the waveguides, since any small lateral deviation tends to couple the forward motion to transverse modes – thus destroying the coherence of the superposition state. In the absence of such coupling the interferometer are expected to be able to operate using multiple transverse modes concurrently (Andersson *et al.*, 2002).

2. Ring traps

Ring traps are the simplest topologically non-trivial atomtronic circuit. They normally consist of a tight harmonic confinement in the vertical and horizontal directions and no confinement along the azimuthal direction. The potential for a ring of radius ρ_0 can be written near the trap minimum as $U = \frac{1}{2}m\omega_\rho^2(\rho - \rho_0)^2 + \frac{1}{2}m\omega_z^2z^2$, with m being the mass of the atoms and ω_ρ and ω_z are the harmonic trapping frequencies in the radial and vertical directions respectively. There are two distinct regimes of interest for ring traps: One where the radius of the ring is small enough for the energy or time-scale of the excitations along the circumference of the ring to become important, and one, where the ring is to be viewed more like a circular waveguide.

Early demonstrations of a ring trap focused on the wave-guide regime. Large-scale magnetic traps have been demonstrated, where the shape of the ring was directly defined by the field generating wires, either using micro-fabricated ‘atom-chips’ (Sauer *et al.*, 2001) or large wire structures (Arnold *et al.*, 2006; Gupta *et al.*, 2005) and inductively coupled rings (Pritchard *et al.*, 2012). For polar molecules electrostatic ring-traps have also been demonstrated (Crompvoets *et al.*, 2001).

Small-diameter ring traps can also be generated using purely optical dipole potentials. The first toroidal BEC was created with a painted potential (Henderson *et al.*, 2009). Static approaches to creating rings with optical potentials include using a light-sheet in combination with a Laguerre-Gauss beam (Moulder *et al.*, 2012; Ramanathan *et al.*, 2011; Wright *et al.*, 2000). Persistent currents in spinor condensates were detected in (Beattie *et al.*, 2013). In this case, the imperfection in the potential often do not lead to adverse effects since the superfluid nature of the flow smooths them over. Examples include studies of super-currents (Eckel *et al.*, 2014b; Moulder *et al.*, 2012; Ryu *et al.*, 2014) and Josephson junctions (Ryu *et al.*, 2013; Wright *et al.*, 2013a).

Optical ring lattices suitable for trapping cold and quantum degenerate atomic samples have been generated with Laguerre-Gauss laser beams incident on SLM or manipulated by an Acousto-Optical Modulator (Amico *et al.*, 2014; Franke-Arnold *et al.*, 2007; Henderson *et al.*, 2009). By applying computer assisted optimization algorithms using absorption images of BECs in the dipole potentials, smooth potentials of rings radii and lattice spacings in the range of $100\mu\text{m}$ and $30\mu\text{m}$ respectively have been demonstrated. DMD generated rings lattices of $\sim 40\mu\text{m}$ and lattice spacing of $\sim 4\mu\text{m}$ have been achieved (Gauthier *et al.*, 2016). However, in order to achieve any appreciable tunneling among the lattice wells, such numbers need to be scaled down further.

3. Barriers and beam splitters

The terms “barrier” and “beam splitters” are primarily distinguished by their intended use rather than by underlying function or principles. Borrowing the term from optics, beam splitters are familiar elements, particularly in the context of interferometers, used for coupling a pair of system modes. Barriers are commonly used to define spatially distinct regions, for example, having different potential structures, temperatures, and chemical potentials as is the case in triple-well transistors, for example (Caliga *et al.*, 2016b). Beam splitters have been implemented using both time-dependent and time-independent potentials, whereas barriers are typically implemented with time independent potentials.

Early work on atomtronic beam splitters split magnetically guided atoms utilizing “Y”- or “X”-shaped conductor junctions, resulting in multi-mode splitting (Cassetari *et al.*, 2000; Muller *et al.*, 2000). Coherent beam splitting on an atom chip has been carried out using Bragg diffraction from an optical lattice that is exposed to the atoms in a double-pulsed manner (Diot *et al.*, 2004; Wang *et al.*, 2005). Coherent splitting of stationary Bose condensates produced on atom chips has also been carried out utilizing radio-frequency fields that provide and elegant means of evolving in time a single magnetically generated potential well into a double well and vice-versa (Hofferberth *et al.*, 2006; Kim *et al.*, 2017; Schumm *et al.*, 2005). Of note, the earlier successes in coherent beam splitting utilized time-dependent potentials.

In the framework of atomtronic circuitry there is particular interest in beam splitters that are spatially fixed and time independent. The use of “painted potentials” (Henderson *et al.*, 2009) enabled coherent splitting of a propagating condensate in “Y” junction optical waveguides (Ryu and Boshier, 2015) while beam splitting in crossing optical waveguides has also been carried out using an optical Bragg grating produced by a pair of interfering laser beams located at the waveguide junction (Guarrera *et al.*, 2017).

In contrast to the coherent splitting that is achieved with waveguides coupled by spatial proximity or through

optical gratings, barriers act more like the mirrors and beam splitters of optical systems. Barriers produced using projected blue-detuned laser beams feature a smooth Gaussian profile. Coherent splitting occurs due to tunneling and quantum reflection for atoms with energies below or above the top of the barrier, respectively, within an energy range proportional to the inverse curvature of the barrier at its top (Cuevas and Scheer, 2017). Matter wave propagation across arbitrary arrangements of barriers can be numerically calculated utilizing the impedance method (Gutiérrez-Medina, 2013; Khondker *et al.*, 1988), a technique that borrows wave propagation techniques from electromagnetic transmission line analysis.

Projected optical atomic potentials that affect the center-of-mass motion through AC Stark shifts are limited in size-scale by the wavelength of the projected light. Barriers having sub-wavelength size scales down to less than 50nm have been demonstrated using the nonlinear response of the dark state of a three-level system (Lacki *et al.*; Wang *et al.*, 2018).

Regarding the large variety of approaches in barrier and beam splitter implementation, it is not evident that a single approach has emerged as best suited for atomtronic systems. Rather, the optimum approach is purpose-dependent. What has emerged, however, is that it has proved quite difficult to achieve coherence-preserving barriers or beam splitters using purely magnetic approaches. Either all optical or hybrid magnetic and optical or radio-frequency systems have met with good success.

III. COHERENT EFFECTS IN MESOSCOPIC MATTER-WAVE CIRCUITS

Like their electronic counterparts (Cuevas and Scheer, 2017), atomtronic devices can operate in a regime where quantum interferences play a dominant role. Such a coherent regime is achieved in situations where the typical transport scale, such as the circumference of a ring trap or the length of a mesoscopic section, is larger than the typical decay length of the particles’ correlation function. Phenomena such as Aharonov-Bohm interferences, Bragg reflection on periodic structures or Anderson localization emerge in the transport properties. Quantum coherent transport is deduced from properties of the Hamiltonian describing the atoms inside the conductor, identical to coherent wave propagation in complex media encountered in electromagnetism.

Operating in this regime typically requires low enough temperatures: for Fermi gases, the relevant length scale is $\frac{\hbar v_F}{k_B T}$, where v_F is the Fermi velocity, and for thermal gases it is the thermal de Broglie wavelength. For bosons, the emergence of the condensate below the critical temperature ensures coherence at arbitrarily large distances, making them particularly well suited for the study of coherent transport. The long wavelength dynamics is then efficiently described by superfluid hydrodynamics (see

Sec. III.A.1). Coherence properties are also affected by many-body effects such as the decrease of quasi-particle lifetime and quantum fluctuations. Furthermore, coherence can be reduced by noise, spontaneous emission from lasers or other external disturbances.

In this section, we bridge microscopic models to simple matter-wave circuits. The various model Hamiltonians describing coherent quantum fluids with different features are introduced. We then focus on the persistent current in ring-shape circuits providing both an important figure of merit for the system's coherence and an elementary building block for atomtronic circuits. Finally we present the two-terminal quantum transport and illustrate the specific features emerging from the coherent quantum dynamics.

A. Model Hamiltonians

The many-body Hamiltonian describing N interacting quantum particles of mass m , subjected to an effective magnetic field described by the vector potential \mathbf{A} and confined in the potential V_{ext} reads

$$H = \int d\mathbf{r} \Psi^\dagger(\mathbf{r}) \left[\frac{1}{2m} (-i\hbar\nabla + \mathbf{A}(\mathbf{r}))^2 + V_{ext}(\mathbf{r}) \right] \Psi(\mathbf{r}) + \frac{1}{2} \int d\mathbf{r} d\mathbf{r}' \Psi^\dagger(\mathbf{r}) \Psi^\dagger(\mathbf{r}') v(\mathbf{r} - \mathbf{r}') \Psi(\mathbf{r}) \Psi(\mathbf{r}') \quad (4)$$

where $\Psi^\dagger(\mathbf{r})$ and $\Psi(\mathbf{r})$ are field operators creating or annihilating a bosonic or fermionic particle at the spatial position \mathbf{r} (Mahan, 2013) and $v(\mathbf{r} - \mathbf{r}')$ is the two-body inter-particle interactions. We assume contact interactions $v(\mathbf{r} - \mathbf{r}') = g\delta(\mathbf{r} - \mathbf{r}')$, with $g = 4\pi\hbar^2 a_s/m$ and a_s the s -wave scattering length. \mathbf{A} is an effective gauge potential, which plays a crucial role in the description of currents in spatially closed geometries. Both lattice and continuous systems are relevant for atomtronic circuits. The quantum many-body theories will be presented mostly for the one-dimensional case. They will be used to describe quantitatively tightly confined geometries, such as quantum wires and point contacts, but also capture qualitatively the physics of extended systems along the transport direction. Given their relevance for specific atomtronic circuits, the Gross-Pitaevskii mean field theories will be discussed also for higher dimensions.

1. Bosons

In this case the field operators obey the commutation relations $[\Psi(\mathbf{r}), \Psi^\dagger(\mathbf{r}')] = \delta(\mathbf{r} - \mathbf{r}')$. For a recent review on one-dimensional bosons see (Cazalilla *et al.*, 2011). We start with a lattice theory describing atoms localized in potential wells centered in N_s sites, and expand the field operators in Wannier functions, assumed to be a good basis of eigenfunctions of separated local potential wells: $\Psi(\mathbf{r}) = \sum_{j=1}^{N_s} w(\mathbf{r} - \mathbf{r}_j) a_j$, in which the operators

\hat{a}_j create a single bosonic particle at the site j , $[a_i, a_j^\dagger] = \delta_{ij}$. With the above expression of $\Psi(\mathbf{r})$, the many body Hamiltonian can be recast to the Bose-Hubbard Model (BHM)

$$\mathcal{H}_{\text{BH}} = \sum_{\langle i,j \rangle}^{N_s} \left[-J (a_j a_{j+1} + a_{j+1} a_j) + \frac{U}{2} n_j (n_j - 1) \right], \quad (5)$$

in which we assumed that only atoms in nearest neighbor local wells can appreciably overlap. A ring geometry is assumed, such that $a_{N_s+1}^\dagger = a_1^\dagger$. The parameters in the Hamiltonian are the hopping amplitude $J = \int d\mathbf{r} w^*(\mathbf{r} - \mathbf{r}_i) \left[\frac{1}{2m} (-i\hbar\nabla + \mathbf{A}(\mathbf{r}))^2 + V_{ext} \right] w(\mathbf{r} - \mathbf{r}_{i+1})$ and interaction strength $U = \pi a_s \int d\mathbf{r} |w(\mathbf{r})|^4/m$. The Hamiltonian (5), originally introduced as a lattice regularization of the continuous theory of bosonic fields (Haldane, 1980), provides a paradigmatic model to study Mott insulator-superfluid quantum phase transitions (Fisher *et al.*, 1989). The BHM was extensively used in mesoscopic physics (Fazio and Van Der Zant, 2001). The conditions for the realization of the the BHM in cold atoms systems were identified in (Jaksch *et al.*, 1998), and since then it provides an important scheme in the cold-atoms quantum technology (Bloch *et al.*, 2008). The vector potential $\mathbf{A}(\mathbf{x}, t)$ for neutral matter is an artificial gauge field (Dalibard *et al.*, 2011; Goldman *et al.*, 2014) - see Sect. III.B.1. For sufficiently smooth $\mathbf{A}(\mathbf{x}, t)$ on the atomic scale, the gauge field can be absorbed in the Wannier functions $\tilde{w}(\mathbf{r} - \mathbf{r}_i) = e^{-i\Lambda(\mathbf{r}, t)} w(\mathbf{r} - \mathbf{r}_i) \approx e^{i\Lambda(\mathbf{r}_i, t)} w(\mathbf{r} - \mathbf{r}_i)$ with $\Lambda(\mathbf{r}, t) = \int_{\mathbf{r}_0}^{\mathbf{r}} \mathbf{A}(\mathbf{r}, t) d\mathbf{r}$, where \mathbf{r}_0 is an arbitrary lattice site. Therefore the hopping parameter results

$$J = e^{i\Phi} J_0, \quad \Phi = \int_{\mathbf{r}_i}^{\mathbf{r}_{i+1}} \mathbf{A}(\mathbf{r}, t) d\mathbf{r} \quad (6)$$

The procedure of absorbing the effects of the gauge field into the hopping matrix element is called Peierls substitution (Essler *et al.*, 2005; Peierls, 1933).

In the limit of a large average number of particles per site $\nu = N/N_s \gg 1$ the Bose-Hubbard Hamiltonian effectively reduces to the Quantum Phase Model (QPM) (Fazio and Van Der Zant, 2001)

$$\mathcal{H}_{\text{QP}} = -2J_{\text{E}} \sum_{\langle i,j \rangle}^{N_s} \left[\cos(\hat{\phi}_i - \hat{\phi}_j - \Phi) + \frac{U}{2} \sum_{j=1}^{N_s} \hat{Q}_j^2 \right], \quad (7)$$

where $J_{\text{E}} = J N_s$, $\hat{Q}_j = n_j - N/N_s$ is the on-site particle number fluctuations and $\hat{\phi}_j$ the (Hermitian) phase operators (Amico, 2000; Amico and Penna, 2000). The operators satisfy the commutation relations $[\hat{\phi}_i, \hat{Q}_j] = i\hbar\delta_{ij}$.

In the limit of small filling fractions $\nu = N/N_s \ll 1$ the lattice Hamiltonian Eq.(5) leads to the Bose-gas continuous theory. This statement holds true since the filling is proportional to the lattice spacing Δ : $\nu = D\Delta$, with D being the particle density. In order to have a

well defined result in the continuous limit $\Delta \rightarrow 0$, the bosonic operators must be rescaled: $\hat{a}_i = \sqrt{\Delta}\Psi(\mathbf{r}_i)$, $\hat{n}_i = \Delta\Psi^\dagger(\mathbf{r}_i)\Psi(\mathbf{r}_i)$, $\mathbf{r}_i = i\Delta$. The BHM reads as (Korepin *et al.*, 1997): $H_{BH} = t\Delta^2\mathcal{H}_{BG}$, $\mathcal{H}_{BG} = \int d\mathbf{r} [(\partial_{\mathbf{r}}\Psi^\dagger)(\partial_{\mathbf{r}}\Psi) + c\Psi^\dagger\Psi^\dagger\Psi\Psi]$, with $c = U/(t\Delta)$ (Amico and Korepin, 2004). This coincides with Eq. (4) where $c = mg/\hbar^2$. We note that while the procedure is valid for any U , the attractive case demands smaller values of Δ for the actual mapping of the spectrum (Oelkers and Links, 2007). This feature is due to formation of quantum analog of bright solitons (Naldesi *et al.*, 2019b).

The many-body Hamiltonian arising from \mathcal{H}_{BG} in first quantization is known as the Lieb-Liniger model and reads

$$\mathcal{H}_{LL} = \sum_{j=1}^{N_p} \frac{\hbar^2}{2m} \left(-i\frac{\partial}{\partial x_j} - \frac{\Phi}{2\pi N_s} \right)^2 + g \sum_{1 \leq j < k < N_p} \delta(x_j - x_k). \quad (8)$$

We note that, despite the Bose-Hubbard model is not integrable (Amico and Korepin, 2004; Choy and Haldane, 1982; Dutta *et al.*, 2015), the 1D Bose gas is, with exact solution given by Lieb and Liniger using the Bethe Ansatz (Lieb and Liniger, 1963).

With a fully factorized (not-entangled) Ansatz for the many-body wavefunction $\Psi_{GS}(\mathbf{r}_1, \dots, \mathbf{r}_N) = (1/N) \prod_j^N \phi(\mathbf{r}_j)$ the dynamics entailed by the Hamiltonian (4) reduces to the Gross-Pitaevskii equation (Calogero and Degasperis, 1975; Dalfovo *et al.*, 1999; Leggett, 2006)

$$i\hbar\partial_t\phi(\mathbf{r}, t) = \left[\frac{\hbar^2}{2m} (-i\nabla - \mathbf{A})^2 + V_{ext}(\mathbf{r}) \right] \phi(\mathbf{r}), \quad (9)$$

$$+ gN |\phi(\mathbf{r})|^2 \phi(\mathbf{r}), \quad (10)$$

in which we restored the 3D character of the system since many relevant applications of the GPE occur in circuits of higher dimensionality (e.g. toroidal confinements). We note that $\sqrt{N}\phi(\mathbf{r})$ coincides with $\langle \Psi(\mathbf{r}, t) \rangle$, defined by the mean field approximation of the Heisenberg equations of the motion stemming from the Hamiltonian Eq. (4). The reduction of the quantum many body problem to the GPE dynamics is well justified in the dilute regime, i.e. when $a_s^3\rho \ll 1$ (see (Lee *et al.*, 1957) for corrections). In 1d, taking $A = 0$ and $V_{ext} = 0$ the Gross-Pitaevskii equation is integrable, with solitonic solutions (Faddeev and Takhtajan, 2007). Eq. (10), recast in amplitude phase representation $\phi = \sqrt{n}e^{i\theta}$ gives rise to the superfluid hydrodynamics equations for the condensate density n and the phase θ (Dalfovo *et al.*, 1999).

2. Fermions

Here, we refer to a gas of fermions with κ spin components. In this case, the field operators are characterized by the spin label $\alpha = \{1, \dots, \kappa\}$. They obey the anti-commutation rules: $\{\Psi_\alpha(\mathbf{r}), \Psi_{\alpha'}^\dagger(\mathbf{r}')\} = \delta_{\alpha,\alpha'}\delta(\mathbf{r} - \mathbf{r}')$.

By employing a similar derivation as described above for the bosonic case, one can obtain the generalization of the Hubbard model. For $\kappa = 2$ the latter provides a paradigmatic framework to address the physics of itinerant two-spin-components fermions, ie electrons, in d -dimensional lattice (Gutzwiller, 1963; Hubbard, 1963; Kanamori, 1963). See (Baeriswyl *et al.*, 2013; Mahan, 2013; Mielke, 2015) for more recent references. The Hamiltonian for $SU(N)$ fermions in a ring lattice pierced by an effective gauge field reads (Capponi *et al.*, 2016)

$$\mathcal{H}_{SU(N)} = -J \sum_{j=1}^{N_s} \sum_{\alpha=1}^{\kappa} (e^{i\Phi} c_{\alpha,j}^\dagger c_{\alpha,j+1} + \text{h.c.}) + U \sum_{\alpha \neq \alpha' j} n_{\alpha,j} n_{\alpha',j} \quad (11)$$

where $c_{\alpha,j}^\dagger$ creates a fermion at the site j of a d -dimensional lattice with spin component α , $n_{\alpha,j} = c_{\alpha,j}^\dagger c_{\alpha,j}$ is the local number operator for site j and spin component α . The parameters J and U account for the hopping strength and on-site interaction respectively. They can be expressed in terms of integrals of Wannier functions as discussed for the bosonic case. Systems of two spin components (Jördens *et al.*, 2008), and more recently, of κ components fermions (Cappellini *et al.*, 2014; Pagano *et al.*, 2015) have been experimentally realized with the cold atoms quantum technology. For $\kappa = 2$, the Hamiltonian (11) is integrable by Bethe Ansatz for any values of system parameters and filling fractions $\nu = N/L$ (Lieb and Wu, 1968). For $\kappa > 2$, the Bethe Ansatz integrability is preserved in the continuous limit of vanishing lattice spacing, (11) turning into the Gaudin-Yang-Sutherland model describing $SU(\kappa)$ fermions with delta interaction (Sutherland, 1968); such regime is achieved by (11) in the dilute limit of small fillings fractions. Bethe Ansatz solutions allows the precise understanding both of the ground state and the nature of excitations of the system. The corresponding Hamiltonian reads:

$$H_{GYS} = \sum_{\alpha=1}^{\kappa} \sum_{j=1}^N \frac{\hbar^2}{2m} \left(-i\partial_{x_{j,\alpha}} - \frac{\Phi}{2\pi N_s} \right)^2 + g \sum_{1 \leq i < j \leq N} \sum_{\alpha, \beta=1}^{\kappa} \delta(x_{i,\beta} - x_{j,\alpha}) \quad (12)$$

Another integrable regime of (11) is obtained for $\langle \sum_{\alpha} n_{\alpha,j} \rangle = 1 \forall j$ and large repulsive values of $U \gg t$ for which the system is governed by the $SU(\kappa)$ antiferromagnetic Sutherland model (Capponi *et al.*, 2016; Guan *et al.*, 2013; Sutherland, 1975). In the intermediate interactions and intermediate fillings, the model (11) for $\kappa > 2$ is not integrable and approximated methods are needed to access its spectrum. $SU(2)$ and $SU(\kappa)$ fermions enjoy a different physics. For spin one-half fermions, spin excitations, the so called spinons, are gapless in thermodynamic limit; charge excitations, instead, are gapped at half filling (Mott phase) and gapless otherwise (Andrei,

1995). In the low energy limit, spin and charge excitations separate each other. Notably, the Mott phase is suppressed only exponentially for $\kappa = 2$ (Lieb and Wu, 1968). For $\kappa > 2$, fermions display a Mott transition for a finite value of U/J (Cazalilla and Rey, 2014; Manmana *et al.*, 2011). For incommensurate fillings, a superfluid behavior is found. In the $SU(\kappa)$ case, spin and charge excitations can be coupled (Affleck, 1988).

To close the section, we mention that relevant many-body quantum systems can be realized by resorting to the notion of synthetic dimension that was recently experimentally implemented by using cold atoms quantum technology. The main idea expressed by the synthetic dimension is to consider suitable degrees of freedom of the particles' system that can layer the dynamics of the system as a true spatial dimensions (Boada *et al.*, 2012; Celi *et al.*, 2014). Examples of synthetic dimension can be achieved through coupled internal (hyper-fine) atomic states. The crucial requirement here is that each internal state is coupled to only two other states in a sequential way. For cold atoms, this can be achieved by suitable Raman coupling between the different internal states. This approach allow to study dimensionality effects (even beyond three dimensions) with enhanced control and flexibility. This way, many-body systems with exotic physical conditions have been explored. Examples include alkaline-earth atoms realizing bosonic ladders in various conditions of gauge fields and spin-orbit couplings (An *et al.*, 2018; Buser *et al.*, 2020; Marchukov *et al.*, 2018) or topological matter (Ozawa and Price, 2019).

3. Impurities, weak-links and contacts

Barriers, weak-links, quantum impurities and contacts are essential features for matter-wave circuits. Most, if not all, of these features can be experimentally realized, with a wide range of parameters both in the spatial and time domains. Below, we will sketch on how they can be incorporated in the systems Hamiltonian.

In continuous systems (like Eqs. (8), (10), (12)), ideal localized barriers can be modeled as delta-function potentials. They can be used to stir ring-shape condensates (Hallwood *et al.*, 2007, 2010; Nunnenkamp *et al.*, 2011; Schenke *et al.*, 2011). In numerical simulations describing closely the experimental conditions the delta function is replaced by a suitably peaked Gaussian function (Nunnenkamp *et al.*, 2011). Localized barriers in lattice systems are achieved through weak-links in the hopping amplitudes (Aghamalyan *et al.*, 2016; Amico *et al.*, 2014) or by suitable offsets of the local potentials (Aghamalyan *et al.*, 2015; Cominotti *et al.*, 2015).

In a typical transport set-up, the effect of a thin localized barrier of large strength can be described by the tunnel Hamiltonian $\mathcal{H} = \mathcal{H}_L + \mathcal{H}_R + \mathcal{H}_t$ in which \mathcal{H}_L and \mathcal{H}_R are the left and right leads, and \mathcal{H}_t is the tunneling Hamiltonian. A standard expression for \mathcal{H}_t is $\mathcal{H}_t = \mathcal{J}(\psi_L^\dagger \psi_R + h.c.)$, ψ_L and ψ_R being single particle

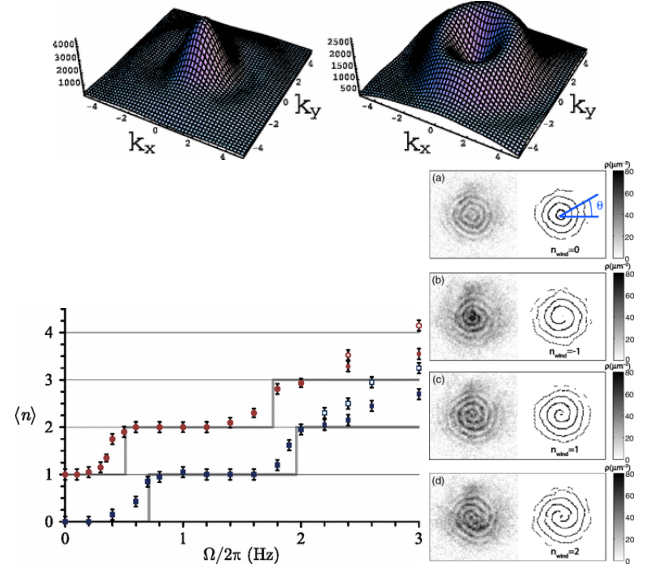


FIG. 5 a) Theoretical prediction of time-of-flight image of current-carrying states from a ring trap. Figure from (Amico *et al.*, 2005) b) Experimental demonstration of persistent currents steps, observed in ultracold atom rings. Figure from (Wright *et al.*, 2013a) c) Measured spiral interferograms to infer sign and quantum number of circulating states on ultracold atomic rings. Figure from (Corman *et al.*, 2014), subpanels a) to d) provide examples of detection of different current states.

operators of the left and right leads respectively (see for example (Nazarov and Blanter, 2009)) and \mathcal{J} the tunnel amplitude. At a semi-classical level, the two leads transport can be described in terms of the atoms transfer among the reservoirs $\Delta N = N_L - N_R$. Specifically, the current is defined as $I = -(1/2)d(\Delta N)/dt$. Such a logic is applied in the two-terminals transport set-ups discussed in the Sect.III.C. In there, transport in open matter wave circuits is studied through standard master equations (Breuer and Petruccione, 2002).

B. Persistent currents in atomtronic circuits

Even though persistent currents are mesoscopic in nature, they are instrumental for atomtronics. They can provide an important tool for quantum simulation, since they can probe quantum phases of matter. At the same time, persistent currents can be used for atomtronic devices such as, e.g. quantum sensing (see Sect.IV.D) or neutral currents-based platforms for qubit implementations (see Sec.IV.C).

1. The concept of persistent current

The persistent current is one of the defining notions of mesoscopic physics (Büttiker *et al.*, 1983; Imry, 2002; Imry and Landauer, 1999): in an electronic ring-shaped gas (a metal for example) pierced by a static magnetic

field, a dissipationless current can occur. This is a manifestation of the electron phase coherence all along the ring, implying that the coherence length is larger than the system size. This counter-intuitive phenomenon occurs in the quantum regime, when resistive effects due to interactions, presence of impurities and thermal fluctuations leading to decoherence are negligible. Persistent currents were thoroughly studied mesoscopic physics both theoretically and experimentally (see eg (Saminada-yar *et al.*, 2004; Zvyagin and Krive, 1995) and references therein), with the aim of shedding light on its own mechanism, studying the effect of interactions, understanding the role of the impurities (Chakraborty and Pietiläinen, 1994; Imry, 2002; Matveev *et al.*, 2002; Riedel and von Oppen, 1993).

In superconductors and superfluids, the persistent currents coincide with the supercurrents flowing across the ring and originate from the macroscopic phase coherence of such quantum states. Experimental observations of persistent currents were reported in several condensed-matter systems: normal metallic rings (Bleszynski-Jayich *et al.*, 2009; Lévy *et al.*, 1990; Mohanty, 1999) and superconductors, (Deaver and Fairbank, 1961). Exciton polaritons have also been proposed as platform to study persistent currents under controllable conditions (Gallemi *et al.*, 2018; Li *et al.*, 2015; Lukoshkin *et al.*, 2018; Sanvitto *et al.*, 2010).

By virtue of the control and flexibility of their operating conditions and the possibility to deal with different particles' statistics, ultracold atoms provide an ideal platform to study persistent current with a new scope. The study of persistent currents was first initiated with synthetic gauge fields in cold atoms systems confined to ring-shaped potentials (Amico *et al.*, 2005). Indeed, a quantum gas in ring-shaped confinement and subjected to an artificial gauge field with flux Φ (see Sect. III.A) behaves as a charged particle subjected to a magnetic field. The artificial magnetic field can be engineered by a variety of techniques in quantum technology ranging from a simple rotation to the transfer of angular momentum through two-photon Raman transitions or Berry phases and hologram phase imprinting techniques (Dalibard *et al.*, 2011; Goldman *et al.*, 2014). The effective magnetic field imparts a phase gradient on the particles' wave function defining a finite velocity field along the ring. For sufficiently smooth guides (i.e. the most common situation in cold-atom experiments) the particles' flow is dissipationless. The current is obtained from the free energy thanks to a thermodynamic identity deduced from the Hellmann-Feynman theorem $I = -(1/2\pi)\partial F/\partial\Phi$ (Zvyagin and Krive, 1995). In the ground-state, the persistent current is $I = -(1/2\pi)\partial E_{GS}/\partial\Phi$.

In the quantum-coherent regime, the particle current is predicted to be a periodic function of the applied flux $\Phi = \omega R^2$ of the artificial gauge field, R being the ring radius. A theorem due originally to Leggett (Leggett, 1991) shows that for spinless fermions and bosons with repulsive interactions on a clean ring, the persistent cur-

rents do not depend on the interaction strength, but merely reflect angular momentum conservation along the ring, so that the ground-state energy is written as $E = E_0(\ell - \Phi/\Phi_0)^2$, with ℓ denoting the z -angular momentum quantum number, i.e. the ground-state energy is piece-wise parabolic and each parabola indicates a different value of angular momentum carried by the circulating particles. The period of oscillation of the currents is the flux quantum $\Phi_0 = \hbar/m$. Inclusion of localized impurities or of a barrier mixes the angular momentum states, thus smoothing the amplitude of the persistent currents (Cominotti *et al.*, 2014; Hekking and Glazman, 1997; Matveev *et al.*, 2002). From the quantum impurity viewpoint, the interacting fluid feels an effective barrier, described as a static impurity. The way the barrier strength is renormalized by the fluid depends on interaction regimes. For repulsive interactions, the Luttinger liquid paradigm (Giannouchi, 2003) holds at intermediate and strong interactions and the effective barrier depends on a power law with the ring size, while for the weak interactions, the barrier is screened by healing length effects (Cominotti *et al.*, 2014). The regime where the barrier effectively splits the ring into two disconnected parts is a universal function of barrier and interaction strength (Aghamalyan *et al.*, 2015). For attractive interactions, the excitation spectrum is quadratic and a universal scaling with a non-trivial interplay of barrier and interaction strength is observed in some interaction regimes (Polo *et al.*, 2020).

Machine learning engineering of persistent currents has been carried out (Haug *et al.*, 2021). Relying on the enhanced capabilities of the DMD, the engineering is achieved by training a deep-learning network on the local potential off-sets thereby trapping the atoms in ring-shaped circuit with lumped parameters Eqs. (5), (7). This approach predicts that there is better performances in the state preparation and in the very nature of persistent currents can be achieved, compared with the existing protocols: the superposition of currents with any two angular momentum states can be prepared and superseding stirring protocols. In addition, currents involving three angular momentum can be engineered. Superposition of two current states have also been proposed as sensors for artificial gauge fields and interactions (Pelegrí, 2018).

Beyond one-dimensional regime, persistent currents were also studied in bosonic ring ladders (Haug *et al.*, 2018a; Polo *et al.*, 2016; Victorin *et al.*, 2019, 2018). There, discrete vortex structures can occur in the transverse direction, giving rise to a wealth of phases (see eg for a review (Amico *et al.*, 2020)). Coupled rings provide an ideal geometry to study Josephson oscillations (Lesanovsky and von Klitzing, 2007; Nicolau *et al.*, 2020). Persistent currents have also been studied in multi-component mixtures, where the criterion of stability and the Rényi entropies were addressed (Abad *et al.*, 2014; Anoshkin *et al.*, 2013; Spehner *et al.*, 2021).

In a three-dimensional ring geometry, many sources of decay of persistent currents have been identified: gen-

eration of elementary excitations, thermal fluctuations, vortices and vortex rings (Abad, 2016; Mathey *et al.*, 2014; Piazza *et al.*, 2009; Wang *et al.*, 2015; Xhani *et al.*, 2020). For a tightly confined ring, persistent currents may still decay by phase slippage mechanisms, in particular through incoherent or coherent phase slips depending on interaction and temperature regimes (Danshita and Polkovnikov, 2012; Kunimi and Danshita, 2017; Polo *et al.*, 2019).

2. Experimental observation in ultracold atom setups

Rotating fluids and persistent currents were also observed in ultracold atomic gases on a ring in a donut-shaped ring trap (Moulder *et al.*, 2012; Ramanathan *et al.*, 2011; Ryu *et al.*, 2014; Wright *et al.*, 2013a). A challenge to rotate a quantum fluid is the generation of excitations and vortices (Arabahmadi *et al.*, 2021; Dubessy *et al.*, 2012). The threshold for creation of excitations has been measured (Wright *et al.*, 2013b). The decay of persistent currents due to thermal fluctuations has been also experimentally studied (Kumar *et al.*, 2017). Recent experiments have also achieved very high rotation quantum numbers, with a rotation speed up to 18 times the sound velocity (Guo *et al.*, 2020; Pandey *et al.*, 2019).

By introducing two moving weak links on the ring in opposite directions, the transition from superfluid to resistive flow was studied (Jendrzejewski *et al.*, 2014). This experiment provides a new technique: the use of a ring to address mesoscopic transport properties (see also Sec. III.C). Along the same line, it was demonstrated that it is possible to study the current-phase relation of a superfluid using a ring geometry (Eckel *et al.*, 2014a).

Persistent currents can be explained with the various branches of the energy dispersion relation as a function of the flux or the rotation rate. In Ref. (Eckel *et al.*, 2014b), hysteresis among different branches was observed and proposed as a method to control an atomtronics device.

3. Readout of the current state

Readout of the currents in ultracold atomic systems can be done in various ways. The time-of-flight images in the plane of the ring, after releasing the atoms from the ring, are predicted to display characteristic shape in which the density around \mathbf{k} is suppressed. The TOF image (taken from the top of the expanding condensate, along the falling direction) shows a donut shape, with a radius proportional to the circulating current (Amico *et al.*, 2005; Moulder *et al.*, 2012; Ryu *et al.*, 2014; Solenov and Mozyrsky, 2010) which is very different from a bell-shaped image in absence of circulation. This has also been thoroughly analyzed in experiments (Murray *et al.*, 2013; Ryu *et al.*, 2014).

An important readout of the current state of the sys-

tem is provided by heterodyne phase detection protocol (Corman *et al.*, 2014; Eckel *et al.*, 2014a; Mathew *et al.*, 2015). In this case, the ring is released and made to interfere with an expanding reference disk. The resulting image shows a characteristic spiral interferogram whose details (number of arms and sense of rotation) depend on the direction of circulation of the currents. The spiral interferograms are also sensitive to the possible phase fluctuations along the ring (Corman *et al.*, 2014; Roscilde *et al.*, 2016): in this case, they display dislocations associated to phase slips. For correlated systems on lattices, the phase information can be achieved by studying noise correlations in the expanding density (Haug *et al.*, 2018b). We finally mention that a minimally invasive technique based on Doppler shift of the phonon modes of the condensate has been demonstrated to be effective to measure the winding number (Kumar *et al.*, 2016b).

4. Persistent current in fermionic rings

Persistent currents occur both in bosonic and fermionic systems with noticeable differences associated to the quantum statistics of the particles and the interactions among its constituents. The first analysis of the fermionic persistent current was carried out in (Amico *et al.*, 2005). In this study, the fermions are described by the one dimensional Hubbard model with twisted boundary conditions. In the case of fermionic statistics, a major effect on persistent currents is the parity effect: the currents behave diamagnetically or paramagnetically depending on the parity of the number of particles on the ring. The effect is due to the imposition of periodic boundary conditions on the wavefunction on the ring. Explicit calculation within bosonization shows the subtle effects of interactions and the effect of temperature (Loss, 1992). There is a temperature scale for the disappearance of the oscillations of the current as $k_B T = \hbar^2 m R^2$. In the case of interacting bosons, no parity effect occurs. In this case, the response is always paramagnetic (Pecci *et al.*, 2020). Readout of current states by interferometric means for fermions requires some attention (Pecci *et al.*, 2021) as compared to the bosonic case since all fermionic orbitals contribute to the interference pattern, giving rise to dislocations in the spiral interferograms. Also, the time-of-flight images of circulating current states display a hole only if the circulating current is large enough to displace the whole Fermi sphere in momentum space (Pecci *et al.*, 2021). In the case when attractive interactions occur among the particles, pairing or formation of higher-order bound states (quartets, many-body bound states) directly affects the persistent currents (Byers and Yang, 1961): the periodicity of the persistent currents scales as Φ_0/n where n is the number of bound particles (Naldegi *et al.*, 2019a). The curvature of the free energy at zero flux also displays a parity effect (Waintal *et al.*, 2008): in this case, it arises from a new branch in the ground-state energy (Pecci *et al.*, 2020). Similar to attractive

bosons, the periodicity of the persistent current of repulsive fermions in the strongly correlated regime is reduced by $1/N$. This effect was demonstrated through Bethe ansatz analysis for SU(2) (Yu and Fowler, 1992) and SU(N) Fermi gases (Chetcuti *et al.*, 2020). Such behavior is due to the remarkable phenomenon of spinons-production in the ground state: spinons compensate the increasing effective flux; since the spinons are quantized and the magnetic flux changes continuously, the compensation can be only partial. Therefore, an energy oscillations with characteristic periods smaller than the bare flux quantum Φ_0 is displayed. We note that the effective attraction from repulsion, detected by the reduced flux quantum, arises because of the spin-spin correlations. This should be contrasted with $1/N$ reduction of the ground state periodicity found in strongly correlated attracting bosons occurring as result of formation of N -particle bound states in the ‘charge’ quasi-momenta (Naldesi *et al.*, 2019a). We finally note that, despite persistent current is mesoscopic in nature, it was demonstrated to display critical behaviour in undergoing quantum phase transitions (Chetcuti *et al.*, 2020). This feature empower atomtronic circuits as current-based emulators in which the matter-wave current is employed as diagnostic tool to probe quantum phases of matter.

The first experimental demonstration of persistent current states in fermionic rings have been reported (Cai *et al.*, 2021).

C. Two terminal quantum transport in cold atom mesoscopic structures

The description in terms of lump elements has a deep counterpart for the description of devices operating in the quantum mechanical regime: a *mesoscopic* region, eg a channel or a ring, is described by quantum physics, and large leads are connected to it to drive currents (Imry and Landauer, 1999). The mesoscopic region features quantum mechanical processes such as tunneling and interferences, while the leads are characterized by their thermodynamic phases, which can be normal or superfluid.

1. Double well systems

Two-terminal systems for cold atoms have first been considered for Bose-Einstein condensates as a way to observe and manipulate phase coherence (Andrews *et al.*, 1997) (see (Dalfonso *et al.*, 1999) for a detailed review). Conceptually, the simplest instance is a zero-temperature BEC in a double well potential, as first proposed in (Smerzi *et al.*, 1997). This system is of considerable interest from many point-of-view, from quantum metrology (Pezzè *et al.*, 2018) to quantum information processing (Haroche and Raimond, 2006). We restrict the discussion to atomic transport and refer the reader to these reviews for in-depth discussions of these other aspects.

a. Tunnel regime In this case, we focus on the dynamics of the population imbalance in the two wells (Smerzi *et al.*, 1997). Such a description is feasible for a high barrier (LeBlanc *et al.*, 2011; Spagnoli *et al.*, 2017). In the unbiased, non-interacting regime, the dynamics reduces to Rabi oscillations of the population across the barrier at the tunnel period, and has been demonstrated experimentally in non-interaction condensates (Spagnoli *et al.*, 2017). For increasing interactions and weak population imbalance, Rabi oscillations smoothly evolve into plasma oscillations, with a frequency controlled by the repulsion between atoms (Albiez *et al.*, 2005; LeBlanc *et al.*, 2011; Levy *et al.*, 2007; Pigneur *et al.*, 2018). For larger population imbalance, the tunneling cannot compensate the effect of the non-linear interaction, leading to macroscopic quantum self trapping. Therefore the population imbalance between the two wells is unable to relax, and the phase difference increases continuously in an approximately linear fashion (Albiez *et al.*, 2005; Levy *et al.*, 2007; Pigneur *et al.*, 2018; Spagnoli *et al.*, 2017). The above-described Josephson dynamics occurs in the absence of dissipation mechanisms, which is true in the two-mode regime at zero temperature (Gati *et al.*, 2006). An intriguing situation occurs for attractive interactions, where the plasma oscillation mode softens down to zero for finite attraction, realizing a canonical example of quantum phase transition (Trenkwalder *et al.*, 2016).

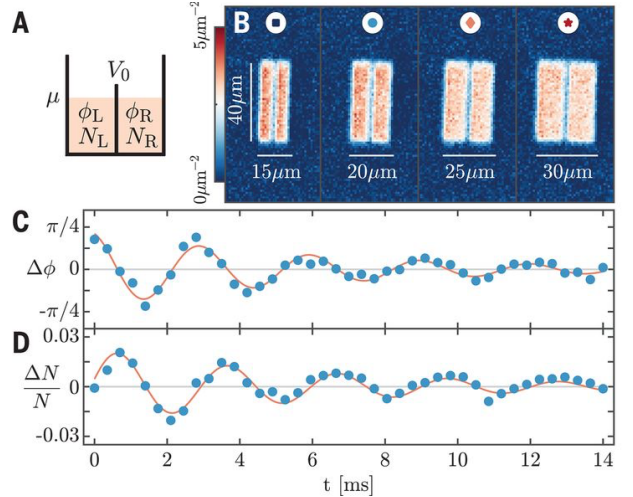


FIG. 6 Josephson junctions imprinted on a strongly interacting two-dimensional Fermi gas (Luick *et al.*, 2020) (A) Sketch of a Josephson junction consisting of two Fermi gases with chemical potential μ , particle numbers $N_{L,R}$, and phases $\phi_{L,R}$ separated by a tunneling barrier. (B) Absorption images of cold atom Josephson junctions. The width of the barrier is held fixed at a waist of $w = 0.81(6) \mu\text{m}$ while the size of the system is increased. (C and D) Time evolution of the phase difference (C) and relative particle number difference (D) between the left and right side of the box after imprinting a relative phase difference of $\pi/4$. The red lines represent a damped sinusoidal fit.

The tunneling and interaction strength parameters of the two-mode model can be derived from the microscopic, mean-field Gross-Pitaevskii equation (Giovanazzi *et al.*, 2008; LeBlanc *et al.*, 2011), and depend on the details of the trap configuration. The predictions of this model are in good agreement with experiment (Ryu *et al.*, 2013). Accounting for fluctuations owing to the discrete nature of atoms allows to describe quantum fluctuations of the phase, similar to phase noise in a non-linear interferometer (Pezzè *et al.*, 2018). Beyond the mean-field approximation in the strongly interacting regime, a rich phenomenology has been predicted (Zöllner *et al.*, 2008). A promising experimental platform for investigating such physics has been demonstrated in (Murmänn *et al.*, 2015) with two atoms and strong correlations. Further quantum effects can also arise also from continuous quantum measurements of the atom numbers (Uchino *et al.*, 2018).

b. Extended reservoirs While the two-mode approximation captures the essence of superfluid atomic currents through a tunnel junction, it disregards some essential processes taking place within the reservoirs. In particular, large reservoirs feature a wide range of excitations that can couple to the current. The double-well structure is a very powerful configuration in which two identical systems can be produced and compared using interferometry. The internal dynamics of each system is then revealed in the phase relation between the two condensates, which has been used to in particular for the study of one-dimensional gases in parallel wire configuration (Betz *et al.*, 2011; Gring *et al.*, 2012; Hofferberth *et al.*, 2007, 2008; Langen *et al.*, 2015). These landmark experiments reveal very fine details of the effective field-theory describing the one-dimensional reservoirs, including high-order correlations (Schweigler *et al.*, 2021). Interestingly, allowing for a finite tunnel coupling between the two reservoirs modifies the effective Sine-Gordon model describing the low-energy physics (Gritsev *et al.*, 2007). In head-to-tail geometry (Binanti *et al.*, 2021; Polo *et al.*, 2018; Tononi *et al.*, 2020), corresponding to the realization of the Boundary Sine-Gordon model, the Josephson oscillations are damped by the phonon bath in each wire, realizing the Caldeira-Leggett model.

The Josephson dynamics coupled with that of the reservoirs is captured phenomenologically by the resistively-shunted Josephson junction model (RSJJ) (Tinkham, 2012), inspired from the condensed matter physics context and applied to atomtronics circuits in (Burchianti *et al.*, 2018; Eckel *et al.*, 2016; Luick *et al.*, 2020). In this model, the reservoirs are described by an effective capacitance, corresponding to the compressibility of the gas $C = \frac{\partial N}{\partial \mu_r}$, with μ_r the reservoirs chemical potential and N its atom number, which can be calculated from the equation of state of the gas and the geometry.

Large reservoirs are also described by a kinetic inductance, arising from the finite mass of the atoms, which

adds to that of the junction to form the total inductance L . The frequency $\omega_0 = (LC)^{-1/2}$ represents the first normal mode of the system, reducing to the dipole mode of in a purely harmonic trap without tunnel barrier or to the plasma frequency in the two-modes model. The tunnel barrier itself is described by its critical current I_c , and the dissipative effects are captured by the parallel 'shunt' resistance R . The superfluid character of the system is encoded in the current-phase relation of the tunnel barrier $I = I_c \sin \phi$ and the Josephson-Anderson equation relating the chemical potential difference $\Delta\mu$ to the phase $\dot{\phi} = \Delta\mu$ (Packard, 1998).

In this framework, the intrinsic properties of the superfluid junction can be studied independently of the dissipation by imposing a quasi-DC current (Kwon *et al.*, 2020; Levy *et al.*, 2007). Alternatively, imprinting a phase difference across the junction by applying an external bias for a short time and measuring the current response through the junction realizes the equivalent of the DC Josephson effect (Luick *et al.*, 2020).

At non-zero temperature, thermally excited atoms are a natural source of dissipation justifying a finite value for R (Levy *et al.*, 2007; Marino *et al.*, 1999; Ruostekoski and Walls, 1998; Zapata *et al.*, 1998). Even at zero temperature, a finite damping arises as the current couples to the internal dynamics of the reservoirs. In weakly interacting BECs and in Fermi gases in the BEC-BCS crossover, the physics captured by the resistance was related to the nucleation of topological defects (Burchianti *et al.*, 2018; Eckel *et al.*, 2016; Jendrzejewski *et al.*, 2014; Valtolina *et al.*, 2015; Wright *et al.*, 2013a; Xhani *et al.*, 2020). In one-dimension, the decay of the current is due to the generation of phase slips, ie space-time vortices (Dubessy *et al.*, 2021; Polo *et al.*, 2019). The current also couples to Bogoliubov excitations in BECs and superfluid Fermi gases as suggested in a two dimensional superfluid Fermi gas at low temperature (Luick *et al.*, 2020; Singh *et al.*, 2020), competing with the coupling to vortices at higher temperature (Singh *et al.*, 2020). The coupling of tunneling with the Bogoliubov spectrum was theoretically studied in (Meier and Zwerger, 2001; Uchino, 2020; Uchino and Brantut, 2020), predicting a finite DC resistance at zero temperature.

Fermi superfluids also feature pair-breaking excitations, which have spectacular effects on the transport properties (Averin and Bardas, 1995). Indirect evidences for such effects have been reported with cold Fermi gases in a point contact (Husmann *et al.*, 2015). Remarkably, the Ambegaokar-Baratoff formula, relating pair-breaking excitations to the critical current in weakly interacting fermionic superfluids was shown to smoothly interpolate with dissipation induced by Bogoliubov excitations in the crossover from BCS to BEC (Zaccanti and Zwerger, 2019). Deeply within the scopes of atomtronics, the Josephson dynamics can be used to probe bulk quantum properties of the materials such as the superfluid order parameter (Kwon *et al.*, 2020) or flat-band superconductivity (Pyykkönen *et al.*, 2021).

c. Weak links in interacting systems In this regime, both the junction and the reservoirs have macroscopic size compared with the coherence or healing length of the underlying gas, the situation is that of a 'weak link' and an appropriate description of transport including in the weak link region can be obtained using superfluid hydrodynamics. Such a description incorporates the transport of non-interacting thermal excitations (Papoulias *et al.*, 2014). A lump element model can be derived from the microscopic hydrodynamics in a rigorous way for weakly interacting bosons, leading to accurate predictions for the dynamics of two-terminal systems (Gauthier *et al.*, 2019). In general, the oscillating character of the populations of the reservoirs (Papoulias *et al.*, 2014) as well as their relationship with the macroscopic phase of the superfluid closely matches the plasma oscillation regime in the two-mode approximation. In these cases, dissipation arises due to phase slippage mechanisms occurring within the weak link, and no qualitative difference emerges for very long channels compared with short tunnel-like barriers (Beattie *et al.*, 2013; Burchianti *et al.*, 2018; Eckel *et al.*, 2016; Jendrzejewski *et al.*, 2014; Wright *et al.*, 2013a; Xhani *et al.*, 2020).

The case of superfluid Fermi gases has been studied in this context through a direct comparison between the unitary gas and a non-interacting Fermi gas, showing two-orders magnitude differences in the conductance (Stadler *et al.*, 2012). Long constrictions or channels can feature sections exposed to a tailored potential, in particular disorder. In a strongly interacting superfluid, a crossover was observed between a low disorder regime with transport dominated by the superfluid character of the gas, and a regime where transport is dominated by strong disorder (Krinner *et al.*, 2013, 2015b).

2. Conductance measurements and incoherent reservoirs

In situations where quantum coherence is either non-existent, or can be neglected such as in junctions dominated by dissipation, transport is captured by the conductance $G = I/\Delta\mu$, where $\Delta\mu$ is the chemical potential difference between the two reservoirs.

a. Non-interacting atoms For reservoirs described by non-interacting particles or quasi-particles, the current is determined by the energy-dependent quantum transmission coefficients of the junction connected to the reservoirs \mathcal{T}_n , where n labels the transverse modes of the junctions, through the Landauer formalism (Cuevas and Scheer, 2017)

$$I = \frac{1}{h} \int d\epsilon \sum_n \mathcal{T}_n(\epsilon) (f_1(\epsilon) - f_2(\epsilon)) \quad (13)$$

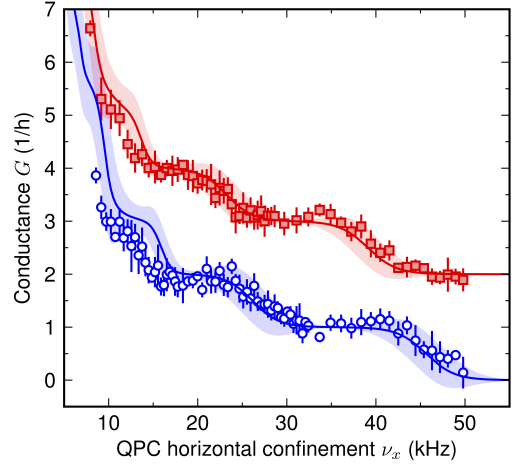


FIG. 7 Observation of quantized conductance in a quantum point contact imprinted onto a weakly interacting Fermi gas (Krinner *et al.*, 2015a). Conductance is measured as a function of the QPC horizontal transverse oscillation frequency (ν_x), for vertical oscillation frequencies of 10.9 and 9.2 kHz (blue and red, respectively). The solid lines show the predictions of the Landauer formula, without adjustable parameter. The shaded areas represent systematic uncertainties on the input parameters. The red curves are offset by two units vertically for clarity.

where f_1 and f_2 are the energy distribution of particles in the two reservoirs. For free fermions and Fermi liquids, f is the Fermi-Dirac distribution corresponding to the reservoir chemical potential μ_i and temperatures T_i . The formalism also applies to weakly interacting bosons above the critical temperature (Kolovsky *et al.*, 2018; Nietner *et al.*, 2014; Papoulias *et al.*, 2016). The strength of the Landauer paradigm is the separation between the quantum coherent part and the incoherent reservoirs, the latter featuring fast dissipation processes that are not described microscopically. The atomtronics Landauer setup, with control over the reservoir properties has motivated detailed theoretical studies of the dissipation processes, by comparing with various microscopic descriptions (Chien *et al.*, 2014; Gallego-Marcos *et al.*, 2014; Ivanov *et al.*, 2013; Kolovsky, 2017; Nietner *et al.*, 2014).

The Landauer paradigm has been proposed for cold atoms in (Bruderer and Belzig, 2012; Gutman *et al.*, 2012) and independently realized experimentally in (Brantut *et al.*, 2012) using a gas of weakly interacting fermions split in two by a mesoscopic, quasi-two-dimensional constriction. For tight constrictions, the system behaves as a simple RC circuit, with capacitors modeling the reservoirs, and the constriction the resistance. Measuring the decay constants of an initially prepared particle-number imbalance between the two reservoirs, and inferring the compressibility from the equation of state allowed to extract the conductance of the constriction. Early experiments focused on variations of conductance induced by changes of shape of the constriction or

the introduction of disorder which were essentially of classical nature (Brantut *et al.*, 2012). In very recent experiments a similar system was used to investigate Anderson localization effects in two dimensions (White *et al.*, 2019).

At zero temperature and low chemical potential difference, Eq. (13) yields $I = \Delta\mu/hj$, j an integer. Each mode energetically accessible in the conductor contributes independently by $1/h$ to the conductance. In experiments, this is manifested in jumps of the conductance by $1/h$ as the Fermi energy reaches the successive transverse modes of the constriction, as observed in condensed matter devices (van Wees *et al.*, 1988; Wharam *et al.*, 1988) and in the atomtronics context (Krinner *et al.*, 2015a).

On top of such an ideal one dimensional conductor, high-resolution optical methods allowed for the projection of structures as described in section II.C.3, such as point-like scatterers. Measuring the conductance as a function of the scatterer's location produced a high resolution spatial map of the transport process, akin to scanning gate microscopy in the condensed matter context (Häusler *et al.*, 2017). Disposing several scatterers in a regular fashion produced a mesoscopic lattice exhibiting a band structure directly observed in the transport properties, demonstrating the ability to observe and control quantum interferences at the single scatterer level (Lebrat *et al.*, 2018).

The notions of reservoirs and channel can also be interpreted in a more abstract way through the concept of synthetic dimension, using internal states of atoms (Celi *et al.*, 2014) or vibrational states of traps (Price *et al.*, 2017). The two-terminal transport concept has also found a generalization through this mapping: a spin imbalanced Fermi gas provides a realization of two terminals in the spin space, and an impurity with engineered spin-changing collisions provide the counterpart of a point contact (You *et al.*, 2019). The use of vibrational states of reservoirs and constrictions as a synthetic dimensions then allows to envision synthetic multi-terminal situations, where transport would be sensitive to chirality (Salerno *et al.*, 2019).

b. Incoherent transport of interacting atoms The situation of quantum point contacts and one dimensional constrictions in the presence of interactions has been heavily investigated in the condensed matter physics context (Imry, 2002), where it has played a crucial role in the development of quantum nano-electronic devices (see for example (Cuevas and Scheer, 2017)). For atomtronics systems in the two-terminal configuration, this situation has been envisioned theoretically for bosons in (Gutman *et al.*, 2012) with ideal reservoirs and in (Simpson *et al.*, 2014) with superfluid reservoirs, in the framework on Luttinger liquid physics. For fermions, the point contacts and wires have been investigated experimentally in the deep superfluid regime for a unitary Fermi gas (Husmann *et al.*, 2015), showing non-linear current-bias rela-

tions that could be traced back to multiple Andreev reflections at the contact, a phenomenon intimately related to pair breaking excitations (Krinner *et al.*, 2017): Because of the point contact, the electron propagates over by a production of a hole propagating back-word. This regime is expected to interpolate continuously with the Josephson regime as the transmission in the point contact is reduced (Averin and Bardas, 1995; Yao *et al.*, 2018). This was further investigated by continuously increasing interactions from the weakly interacting Fermi gas, showing quantized conductance, up to unitarity with non-linear response (Krinner *et al.*, 2016). In the intermediate regime, the conductance plateau was observed to increase continuously from $1/h$ up to values as high as $4/h$ before disappearing close to unitarity. Several interpretations have been proposed for this phenomena, relying either on confinement induced effects inducing pairing within the contact (Kanász-Nagy *et al.*, 2016; Liu *et al.*, 2017) or on superfluid fluctuations in the reservoirs in the normal state contributing to the conductance (Uchino and Ueda, 2017).

Transport in the one dimensional lattice, featuring a band structure, offered the possibility to explore the fate of metallic and insulating behavior as interactions are varied (Lebrat *et al.*, 2018). It was found that the band insulator evolves smoothly into a correlated insulator made of bound pairs with unit filling in the lattice, as interactions are increased up to unitarity, providing evidence for the Luther-Emery phase (Giamarchi, 2003).

c. Spin and heat transport Transport in the two-terminal system can be generalized to spin in a two-component Fermi gas, where the total magnetization is conserved, and can be exchanged between two reservoirs. The linear response in currents is expressed through a matrix relating the currents of the two spin components to their respective chemical potential biases, with off-diagonal elements describing spin drag. In contrast with particle conductance, which is weakly affected by inter-atomic interactions unless superfluidity is approached, magnetization currents are very sensitive to interactions since collisions do not conserve the total spin current. Even in the absence of a constriction or channel, two clouds of opposite polarization relax very slowly to equilibrium especially at unitarity (Sommer *et al.*, 2011), where the spin diffusion coefficient saturates to a universal value. These experiments have been repeated for a metastable, strongly repulsive Fermi gas, providing evidence for a ferromagnetic instability (Valtolina *et al.*, 2017). In the case of a one dimensional quantum wire, the strongly attractive Fermi gas was found to behave as an ideal spin-insulator, as a consequence of pairing (Krinner *et al.*, 2016). Another possibility to manipulate spin currents is open by the use of spin-dependent potentials, that were used to produce a spin valve from a quantum point contact (Lebrat *et al.*, 2019).

Heat and energy transport can be investigated by in-

troducing a temperature bias between the two reservoirs and observing energy flow through the channel. Heat and particle currents couple both through the thermodynamics of the reservoir due to finite dilation coefficients, and through genuine thermoelectric effect originating from the energy dependence of the transmission coefficient, as was observed in (Brantut *et al.*, 2013). This opens the perspective of Peltier cooling methods for quantum gases (Grenier *et al.*, 2014, 2016; Sekera *et al.*, 2016). In the case of the unitary Fermi gas, a similar experiment on quasi-one dimensional constrictions was performed, yielding a low heat conductance and a breakdown of the Wiedemann-Franz law, in qualitative agreement with theory (Pershoguba and Glazman, 2019), but a thermopower compatible with that of a non-interacting Fermi gas (Husmann *et al.*, 2018). Such a breakdown was also predicted for strongly interacting bosons within the Luttinger liquid framework (Filippone *et al.*, 2016).

d. Dissipative barriers One original possibility opened up by cold atomic gases as opposed to electrons in the condensed matter context is the engineering of atom losses. This has been investigated using the electron microscopy, allowing to create highly localized purely dissipative barriers (Barontini *et al.*, 2013; Labouvie *et al.*, 2015). The non-hermitian character of the resulting Hamiltonian allowed for the observation of coherent perfect absorption (Müllers *et al.*, 2018). Using an optical barrier involving spontaneous emission also produces dissipation in addition to the optical potential. This was studied in (Corman *et al.*, 2019). The interplay of these effects with interactions and fermionic superfluidity was investigated in (Damanet *et al.*, 2019a).

3. Two terminal transport through ring condensates

Drain-to-source transmission through circuits with closed architectures provides a direct way to explore the coherence of the system (Imry, 2002). At the same time, it provides an instance for integrated atomtronic circuits (rectilinear and circular guides).

In the simplest implementation, particles are injected from a source lead into ring-shape circuit pierced by an effective magnetic field, and then collected in the drain lead. In such a configuration, the phase of particles couples with the gauge field and transport displays interference patterns characteristic of the Aharonov-Bohm effect (Aharonov and Bohm, 1959; Leggett, 1980; Olariu and Popescu, 1985; Vaidman, 2012), as studied in electronic systems (Büttiker *et al.*, 1984; Gefen *et al.*, 1984; Hod *et al.*, 2006; Jagla and Balseiro, 1993; Lobos and Aligia, 2008; Marquardt and Bruder, 2002; Nitzan and Ratner, 2003; Rincón *et al.*, 2009, 2008; Shmakov *et al.*, 2013; Webb *et al.*, 1985).

Atomtronics allows to study the quantum transport through ring-shaped circuits in new ways, with carriers

of various statistics, tunable atom-atom interactions and lead-ring couplings (Haug *et al.*, 2019a,c; Haug, 2020). Specifically, the non-equilibrium dynamics, described by Bose-Hubbard or discrete Gross-Pitaevskii models, was analyzed by quenching the particles spatial confinement in both closed and open configuration. Depending on the ring-lead coupling, interactions and particle statistics, the system displays qualitatively distinct non-equilibrium regimes characterized by different response of the interference pattern to the effective gauge field. In contrast to a fermionic system, the coherent transport of strongly interacting bosons does not display the characteristic oscillations of the interference fringes as function of the effective magnetic flux. A possible explanation for the suppression of the Aharonov-Bohm oscillations comes as a compensation between the phase of the condensate and Aharonov-Bohm phase. For a field theoretic explanation for the absence of Aharonov-Bohm interference in the circuit see Tokuno *et al.*, 2008.

The transport through lead-ring interface can display an effect that is the bosonic counterpart of the Andreev scattering: a bosonic density wave excitation travelling forward in a one-dimensional condensate with a local discontinuity of interactions can be transmitted with the emission of an excitation with negative amplitude, a 'hole', that is reflected back-word (Daley *et al.*, 2008; Watabe and Kato, 2008; Zapata and Sols, 2009). Two terminal transport through rings and Y-junctions were considered (Haug *et al.*, 2019a). The bosonic Andreev scattering occurs at the lead-ring interface. In addition, the absence of Aharonov-Bohm oscillations in the source-to-drain transmission in the strong lead-ring coupling regime is confirmed.

A coherent transport can also be achieved through topological pumping, by driving periodically in time a system protected by a band gap (Thouless, 1983; Thouless *et al.*, 1982). Such periodic drives are natural within atomtronics, thanks to the availability of re-configurable circuits (Gaunt and Hadzibabic, 2012; Gauthier *et al.*, 2016; McGloin *et al.*, 2003). Topological pumping through source-ring-drain atomtronic circuit was addressed in Haug *et al.*, 2019b. This way, topological bands and Aharonov-Bohm effect in interacting bosonic system are intertwined: the Aharonov-Bohm interference affect reflections by inducing specific transition between topological bands. As a matter of fact, the system works as a non-linear interferometer, in which the source-ring and the ring-drain act as beam-splitter. Interaction adjusts the transmission and reflection coefficients as well as creates entanglement between the propagating wave-function in the two arms of the interferometer.

IV. ATOMTRONIC COMPONENTS AND APPLICATIONS

In this section, we discuss the atomtronic circuital elements that have been discussed in the literature. The first sections concern the atomic counterparts of some circuital elements of classical electronics. Atomtronic qubits inspired by quantum electronics will close the section.

A. Matter wave optics in atomtronic circuits

Transport in atomtronic circuits can be either coherent transmission like in photonic circuits or more like a superfluid similar to superconducting electronics. A classical example is the decay of superfluid currents as described in Sec. III.B. The main stumbling block in observing the coherent transmission of matter waves over macroscopic distances was the roughness of the waveguides that were available.

Until recently, except for straight guides formed by collimated laser beams, atomtronics was limited to the latter. This changed recently with the first demonstration of coherent guiding over macroscopic distances in a ring-shaped matter wave guide (Pandey *et al.*, 2019). It is now possible to (de)accelerate BECs in an optimal way to speeds of many times the critical superfluid velocity and an angular momentum exceeding $40000\ \hbar$ per atom without observable decay over time. Matter-wave lensing or delta-kick cooling (Arnold *et al.*, 2002; Kovachy *et al.*, 2015) has now been demonstrated using gravito-magnetic lenses inside of TAAP matter-wave guides, where BECs and thermal clouds have been collimated, thus reducing their expansion energies by a factor of 46 down to 800 pK (Pandey *et al.*, 2021). Delta-kick cooling with an optical potential is routinely used in waveguide atom interferometers to lower the energy of an expanded and collimated BEC below 300 pK (Krzyzaniowska *et al.*, 2021).

B. Transistors, diodes, and batteries

Semiconductor devices form the backbone of modern electronic circuitry. The semiconductor transistor in particular is a ubiquitous workhorse, with over ten billion in today's state-of-the-art cell phones. One might wonder why the transistor is so pervasive: the answer is that a transistor provides *gain*. The canonical transistor is a three terminal device in which a small current or voltage can control a large current. Starting from this single character of a transistor one can build amplifiers, switches, memory elements, oscillators, logic gates and so on. Thus it is compelling to consider whether atomtronic duals to the transistor and other semiconductor devices can lead to a breadth of application and utility for atomtronics that rivals electronics.

The early work in atomtronic devices sought to emulate semiconductor material-based elements by considering neutral atoms in optical lattices, (Pepino *et al.*, 2009;

Pepino, 2021; Seaman *et al.*, 2007) but work also sought simply functional duals by considering atoms confined to a small number of potential wells (Stickney *et al.*, 2007). There are substantial differences in underlying physics, as well as practical differences, between these two approaches to device design.

Lattice based devices share clear analogies with electronic systems in periodic potentials characterized by band structure effects. At the same time, bosonic many-particles systems are unavoidably characterized by specific quantum correlations making their dynamics very distinct from the electronic one. Specifically, lattice-based atomtronic components deal with superfluids (instead of conductors) and heavily rely on the possibility to engineer a Mott insulating quantum phase that interacting bosons can undergo to, for integer filling fractions (number of bosons commensurate with the number of lattice points). Another effect without any classical electronics analog is the macroscopic quantum self trapping phenomenon that can hinder the transmission of a bosonic fluid through a potential barrier (Milburn *et al.*, 1997; Smerzi *et al.*, 1997). As a specific example of the semiconductor approach, an atomtronic diode can be conceived in analogy with the electronic P-N junction diode: the different concentration of electrons and holes in the P and N materials set a potential drop that can be modulated by an external voltage bias; the so-called forward (reverse) bias corresponds to a reduction of the potential drop for the electrons (holes) at the junction, and therefore the a particles flow take place. In the atomtronic diode, the junction is realized by facing commensurate and incommensurate lattices of condensates; an abrupt change of the chemical potential at the junction, playing the role of the voltage bias (Pepino *et al.*, 2009). This way, the control of the chemical potential can make the bosons from the commensurate to the incommensurate lattice of condensate, but not vice-versa. The diode may be connected to two bosonic reservoirs kept at different chemical potential that play the role of the battery. Ultimately, the nonlinear device behavior arises from the *non linearity* of the atom-atom interactions that is a feature specific to the lattice systems.

We have been nonchalant in referring to the battery in the diode context. It is deeply significant to appreciate that classical electronic circuits are non-thermal-equilibrium systems whose dynamics is wholly driven by the presence of a battery (or other source of electric potential), that is, the battery supplies power to run the circuit. It is also significant to appreciate that a battery is fundamentally associated with an internal resistance, which causes the battery to dissipate energy as it also supplies power to a load. In atomtronic circuits, it is a BEC, having finite chemical potential and temperature, that serves to provide chemical potential and to drive the non-equilibrium dynamics of a circuit. And like the electrical battery, a BEC-based battery providing atom current to a circuit will exhibit an internal resistance. While the classical battery is always associated with a positive

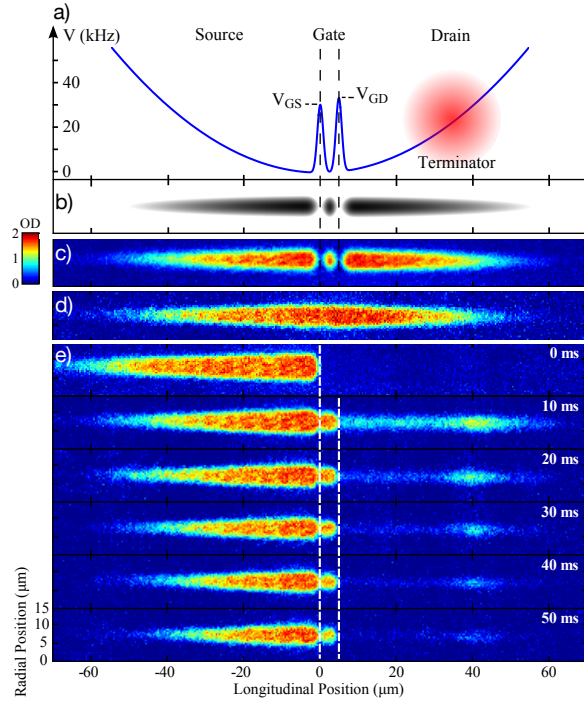


FIG. 8 The atomtronic triple-well transistor. The upper panel a) shows the atomic potential consisting of a hybrid magnetic confinement combined with barriers superimposed by optical projection of a pair of blue-detuned laser beams. A laser beam labeled "Terminator" removes atoms from the drain by pumping them to an untrapped m_F state. The gate width is 4.5μ . b) A density plot of the net magnetic + optical potential shows the structure transverse to the longitudinal axis of the trap. Thermal atoms are loaded in the atomic potential for the sake of visualization of the hybrid potential (c) and in absence of the optical barriers (d). Panels e) and below are absorption images of the atoms in the wells at various evolution times starting from $t = 0$ ms and ending at 50ms. Prior to $t = 0$ a BEC is loaded into the source well, and the optical barriers are lowered to their specified heights to define $t = 0$. These images are taken by allowing the system to evolve for the specified time, but extinguishing the terminator beam 4.8ms before an absorption image is taken. This allow time for the atoms to travel in the drain from the gate to the classical turning point at the right-hand side of the drain potential. As the atoms are moving slowly as they approach the turning point their density is high relative to other locations in the drain. Note that the gate well is initially empty but in fact fills very quickly. Experimental details can be found in (Caliga *et al.*, 2016a, 2012)

resistance, a atomtronic (BEC) battery can exhibit either positive or negative internal resistance, depending on whether the supplied current is thermal or condensed, respectively (Zozulya and Anderson, 2013). An experimental study of atomtronic batteries was carried out in Caliga *et al.*, 2017.

A battery not only powers a circuit, but it is, of course, necessary to provide the gain associated transistor action. Such action has been studied in semi-classical context uti-

lizing a triple-well atomtronic transistor in an oscillator configuration - See Fig. 8 (Caliga *et al.*, 2016b; Stickney *et al.*, 2007). The left-most well acts as source, the middle as gate, and the right as drain, where the nomenclature is taken from the electronic field-effect transistor. Here the system is initialized by placing a BEC at a given temperature and chemical potential in the source well.

The transistor circuit behavior is characterized by a critical feedback parameter given by a normalized difference in barrier height (Caliga *et al.*, 2012):

$$v = \frac{V_{GD} - V_{GS}}{k_B T_S}, \quad (14)$$

where k_B is Boltzman's constant, T_S is the temperature of the source atoms, and V_{GD}, V_{GS} are the barrier heights (see Fig. 8). A theory has been developed using a semi-classical kinetic treatment in which the atoms are treated as particles, while they are also allowed to Bose-condense under appropriate conditions. The treatment reveals that a BEC will spontaneously develop in an initially empty gate well when the feedback exceeds a threshold value (Caliga *et al.*, 2012). This is reflected in the data of Fig. 8 where a high-density of atoms appears in the gate at 10 ms evolution time –in fact the high density is apparent after only 1 ms (Caliga *et al.*, 2012).

The functioning of such a scheme was further studied by analyzing the transport dynamics of the transistor coupled to the environment. In such case the atom steady currents are driven by the chemical potentials with a semi-classical dynamics involving thermal atoms (Caliga *et al.*, 2016b). In particular, by analyzing the gain as function of the operating condition, it was proved that the such atomtronic component can be used to supply power to a given load (therefore acting as an active component). The transport dynamics of the atomtronic transistor was studied experimentally in Caliga *et al.*, 2016a.

C. Atomtronic qubit implementations

Atomtronics qubit implementations have been proposed to combine the logic of cold atoms and superconducting circuits. The basic idea is to use the persistent currents of cold atoms systems flowing in ring shaped potentials; in order to have two well defined energy levels, the translational invariance of the system needs to be broken by the insertion of suitable weak-links. The presence of the weak-link breaks the axial rotational symmetry of the ring fluid and couples different angular momenta states, opening a gap at the degeneracy point among two angular momentum states (see Sec.III.B.1). This way, the two states of the qubit system are the symmetric and anti-symmetric combinations of the two angular momentum states (Aghamalyan *et al.*, 2015, 2016; Amico *et al.*, 2014, 2005; Solenov and Mozyrsky, 2010). The nature of

the superposition state depends on the system parameters: at weak interactions it is a single-particle superposition, at intermediate interaction a NOON-like state and at very strong interactions a 'Moses state' i.e. a superposition of Fermi seas (Hallwood *et al.*, 2006; Nunnenkamp *et al.*, 2008; Schenke *et al.*, 2011).

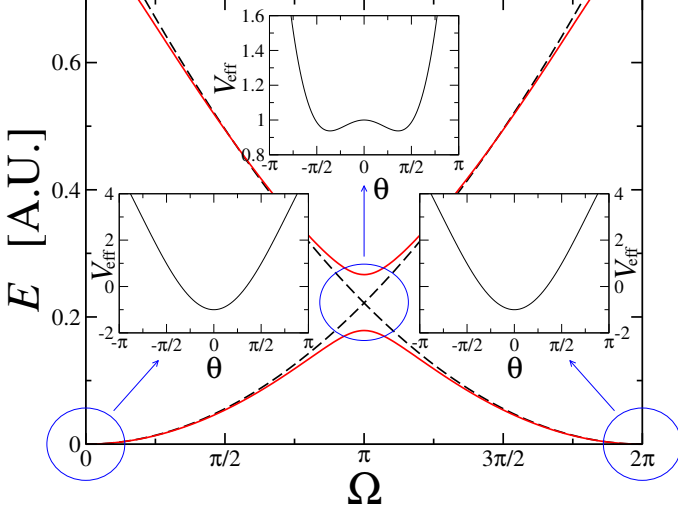


FIG. 9 Main panel: sketch of the qubit energy splitting, due to the barrier Λ , for the two lowest-lying energy states in the many-body spectrum of model (5). Black dashed lines denote the ground-state energy in absence of the barrier, as a function of the flux Ω . Switching on the barrier opens a gap at the frustration point $\Omega = \pi$ (continuous red lines). The three insets show the qualitative form of the effective potential at $\Omega = 0, \pi, 2\pi$ as detailed in the text. Note the characteristic double-well shape forming at $\Omega = \pi$. The qubit, or effective two-level system, corresponds to the two lowest energy levels of this potential. In this figure the energies are plotted in arbitrary units. Taken from (Aghamalyan *et al.*, 2015).

Qubit dynamics exploiting rf-AQUD (Amico *et al.*, 2014) or ring-shaped condensates interrupted by three weak-links (Aghamalyan *et al.*, 2016), in analogy of the Josephson junctions flux-qubits configurations, have been demonstrated theoretically integrating out the all the phase differences among nearest-neighbour condensates except the phase slip across the weak link, the effective dynamics results to be governed by two level system Hamiltonian with potential V_f . An important point in this context, is to establish to what extent the cold-atoms quantum technology would be capable to address the qubit feasibly. In particular, the energy gap separating the two energy levels of the qubit displays a specific dependence on the number of atoms in the ring network, atom-atom interaction and atom tunneling rates through the weak link (Nunnenkamp *et al.*, 2011). The analysis shows that the limit of a weak barrier and intermediate to strong interactions form the most favorable regime to obtain a finite gap between the two energy levels of the double level potential as depicted on Fig. (9) (Aghamalyan *et al.*, 2016; Amico *et al.*, 2014). The spectral quality of the qubit was analyzed in

(Aghamalyan *et al.*, 2015) as function of the physical parameters of the system. The three weak links architecture (Aghamalyan *et al.*, 2016), indeed, realizes a two-level effective dynamics in a considerably enlarged parameter space. Machine learning preparation of entangled persistent current was demonstrated in Haug *et al.*, 2021. The read-out of the qubit has been studied with various expanding condensate protocols (Aghamalyan, 2015; Haug *et al.*, 2018b). In particular, the two-level system structure and the corresponding specific entanglement between the clockwise and anti-clockwise flows can be quantified through the noise in the momentum distribution: $\langle \hat{n}(\mathbf{k})\hat{n}(\mathbf{k}) \rangle - \langle \hat{n}(\mathbf{k}) \rangle \langle \hat{n}(\mathbf{k}) \rangle$ (Haug *et al.*, 2018b). The two states of the qubit could be manipulated through a suitable 'pulse' of artificial magnetic field. A quench protocol, similar in logic to Rabi spectroscopy, was designed to probe the qubit coherent oscillations (Polo *et al.*, 2020; Schenke *et al.*, 2011). This way, qubit gates can be realized (Amico *et al.*, 2014). The read-out of the qubit states have been investigated through the dynamics of expanding condensate (Aghamalyan *et al.*, 2015; Haug *et al.*, 2018b).

Proof of concepts for qubit coupling have been provided in which qubits are imagined to be arranged in stacks (Amico *et al.*, 2014) or in planar (Safaei *et al.*, 2018) configuration. We comment that by relying on recent optical circuit design, much more flexible solutions are feasible to be implemented (Rubinsztein-Dunlop *et al.*, 2016).

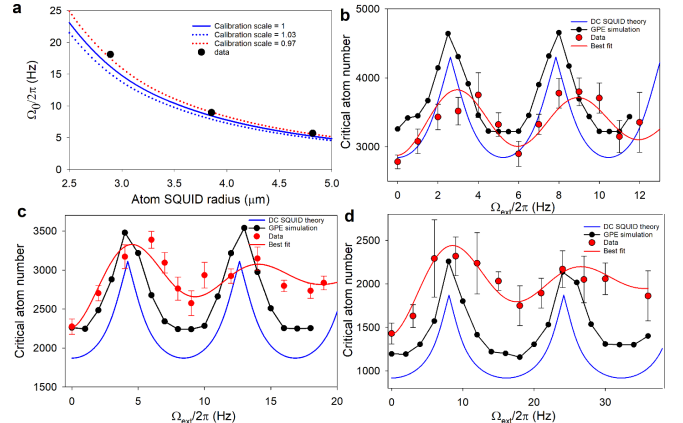


FIG. 10 Comparison between experiment and theory. **a**) Comparison of the measured and calculated values of $\Omega_0/(2\pi)$ (calculation done using GPE). The three curves correspond to calibration scales of the atomtronic SQUID radius. **b,c,d)** Critical atom number as a function of the rotation rates obtained with GPE simulation and DC SQUID theory, along with the measured data and the best fit. For **b**) the radius is $4.82 \mu\text{m}$, for **c**) the radius is $3.85 \mu\text{m}$ and for **d**) the radius is $2.891 \mu\text{m}$. Graph is taken from (Ryu *et al.*, 2020).

Progress to probe the AQUID quantum dynamics has been recently carried out experimentally. Ryu *et al.*, 2020 demonstrated the interference of persistent currents of AQUIDs. By inducing a bias current in a rotating atomic ring interrupted by two weak links, the interference be-

tween the Josephson current with the current from the rotation creates a oscillation in the critical current with applied flux. This oscillation is measured experimentally in the transition from the DC to the AC Josephson effect. This experiment has been performed within a dilute Bose-Einstein condensate that is well described within a mean-field description and thus entanglement of currents, which is a key ingredient for the atomic qubit, has not been demonstrated. Nonetheless, it is a major step towards the implementation of the atomic qubit.

D. Atomtronic Interferometers

An interferometer splits a wavefunction into a superposition of two parts and then recombines them in a phase-coherent fashion. If the wavepackets overlap perfectly at the output of the interferometer, the phase difference between the two arms is difference between the phase shifts imposed by the pulsed beam-splitters and mirrors in each arm plus the propagation phase $\Delta\phi_{prop} = (S^1 - S^2)/\hbar$, where S^i is the classical action computed along path i (Peters *et al.*, 2001). A beamsplitter at the interferometer transforms the phase difference into a population difference, which is easily read out. Most of the atom interferometer solutions demonstrated to date involve freely-falling atoms (Arimondo *et al.*, 2009; Bongs *et al.*, 2019; Geiger *et al.*, 2020, 2011; Müller *et al.*, 2008; Stockton *et al.*, 2011; Sugarbaker *et al.*; van Zoest *et al.*, 2010). Such free fall matter-wave interferometers have the advantage of decoupling the atoms from many effects which otherwise might cause uncontrollable additional phase shifts, which can lead to a deterioration of contrast or a random shift of the fringes. The main disadvantage is the size of the interferometer: Longer interrogation times lead to larger phase shifts. Therefore high-precision matter-wave interferometers need to be very tall in order to accommodate the distance that the atoms fall during the interrogation—reaching a size of ten or even one hundred meters (Kovachy *et al.*, 2015; Muntinga *et al.*, 2013). In contrast to this, atomtronic interferometers use a trapping/guiding potential (usually magnetic or dipole) to compensate gravity and thus can achieve a much increased detection time with much reduced space requirements. This comes, however, at the cost of an increased risk of noise and systematic effects due to fluctuations in the guiding potential.

a. Sagnac effect based atomtronic sensors: An important application of waveguide atom interferometer gyro-technology is inertial navigation in the absence of position information provided by a Global Navigation Satellite System (GNSS). An inertial navigation system (INS) contains three accelerometers, whose output is integrated twice to get displacement, along with three gyros that track the orientation of the accelerometers. It turns out that the navigation accuracy of current INS over

timescales of hours and longer is limited by the drift in the zero of the gyros. These sensors are usually fiber-optic gyros (FOGs). Free-space atom interferometer gyros have already demonstrated extremely low drift (Gustavson *et al.*, 1997, 2000), with their main disadvantage for some applications being the large physical size required to accommodate free fall of atoms being interrogated over several seconds. Guided atom interferometer gyros, analogous to the FOG, would be much more compact, making them attractive for navigation if they can be engineered to have low drift.

In a typical configuration, atomtronic high-precision rotation sensors are based on Sagnac effect: two input quantum waves propagating along two different arms of a closed path circuit (schematically of ring-shape) of enclosed area A produces given interference fringes; if the circuit is put in rotation Ω , the interference fringes results to be shifted. The amount of the shift is

$$\Phi_{\text{Sagnac}} = \frac{4\pi E}{hc^2} \mathbf{A} \cdot \boldsymbol{\Omega} \quad (15)$$

in which E is the energy of the traveling wave, being \mathbf{A} and $\boldsymbol{\Omega}$ the enclosed area and rotation vectors respectively. For frequency ν photon-based Sagnac interferometers $E_{\text{ph}} = \hbar\nu$ and for matter-waves it is $E_{\text{mw}} = mc^2$ instead, yielding $\Phi_{\text{Sagnac}} = \frac{4\pi}{\hbar/m} \mathbf{A} \cdot \boldsymbol{\Omega}$. For equal particle flux and enclosed area, the difference in sensitivity between photon and matter wave interferometers is thus the ratio between the energies $E_{\text{mw}}/E_{\text{ph}} = 10^{10}$. Light-based interferometers typically contain orders of magnitude more photons than the matter wave interferometers contain atoms. They also tend to enclose a much larger area. Nevertheless, matter wave interferometers are expected to outperform their photon counterparts, e.g., where an absolute long-term zero is required.

b. Bright solitons rotation sensors: BEC with attractive interaction (f.i. ^{85}Rb or ^7Li) in ring shaped guides can define a bright soliton interferometry: A localized barrier can split the solitons in two waves propagating in clockwise and anticlockwise that can ultimately recombine after traveling two semicircles. Despite (perfect) bright solitons can go through each other without changing their density shapes, the two waves can provide a Sagnac phase shift (Helm *et al.*, 2015, 2012; McDonald *et al.*, 2014; Polo and Ahufinger, 2013). The scattering properties of a quantum matter wave soliton splitting in a barrier were analyzed (Helm *et al.*, 2014; Weiss and Castin, 2009). Because of the formation of solitons, an enhanced control on the number of atoms N in the experiments is expected. The roles of quantum noise and interaction for rotation sensing with bright solitons in the quantum regime were studied in (Haine, 2018).

The equivalent of bright soliton in the fully quantum regime of a ring lattice of attracting bosons described by Bose-Hubbard attraction was studied (Naldezi *et al.*, 2019b). Because of the lattice the soliton and the number

of atoms is protected by a finite gap. Quantum analog of bright solitons the barrier splitting properties depends on the interplay between interaction, number of particles and barrier strength. In a ring shape confinement, it was demonstrated that the elementary flux quantum is reduced by $1/N$ (Naldesi *et al.*, 2019a). Such an effect potentially yields a N -factor enhancement in the sensitivity of attracting bosons to an external field that can approach the Heisenberg limit (Naldesi *et al.*, 2019a; Polo *et al.*, 2020).

c. Other atomtronic rotation sensors: In (Japha *et al.*, 2007), the analogy between the Sagnac effect for massive neutral particles and the Aharonov-Bohm effect in coherent electron transmission through mesoscopic rings is explicitly employed to propose a new type of rotation-sensitive guided atom interferometer. There are several other proposals for novel types of atomtronic interferometer in the literature (Halkyard *et al.*, 2010; Helm *et al.*, 2015, 2018; Moukouri *et al.*, 2021; Pelegri, 2018).

d. Gravimetry: Atom-interferometers are also expected to excel in gravimetry, where atoms are already starting to outperform their classical counterparts even in the commercial domain. Atomtronics offers highly-sensitive absolute gravimetry at micron size distances and even search for non-Newtonian contributions (Harber *et al.*, 2005).

e. Demonstrated Interferometers: Guided and trapped atom interferometers have been realized in both optical and magnetic traps. One of the earliest examples was a Michelson interferometer using a BEC propagating over $120\ \mu\text{m}$ in a magnetic waveguide on an atom chip (Wang *et al.*, 2005). Smoother waveguides obtained with larger coils have been used to realize atom interferometers with thermal atoms (Qi *et al.*, 2017; Wu *et al.*, 2007) and BECs (Burke *et al.*, 2008; Burke and Sackett, 2009; Garcia *et al.*, 2006). This approach has been used to measure the ground state polarizability of ^{87}Rb (Deissler *et al.*, 2008). In optical waveguides (Akatsuka *et al.*, 2017; Ryu and Boshier, 2015) linear interferometers extending up to $1\ \text{mm}$ have been demonstrated (McDonald *et al.*, 2013b). A number of area enclosing interferometers have been realized in macroscopic magnetic traps (Burke and Sackett, 2009; Moan *et al.*, 2020; Qi *et al.*, 2017; Wu *et al.*, 2007). Recently, an atomtronic Sagnac rotation sensor based on a moving linear waveguide formed by a collimated laser beam was demonstrated (Krzyzanowska *et al.*, 2021). The $3.5\ \text{mm}^2$ enclosed by the atomtronic circuit is the largest value realized to date.

In area-enclosing waveguide atom interferometers the signal can be increased by allowing the wavepackets to make multiple orbits around the waveguide loop to increase the enclosed area. The maximum number of round

trips is usually limited by atom loss when the counter-propagating wavepackets move through each other. It has recently been shown that this limitation can be removed in an interferometer based on a non-interacting ^{39}K BEC, allowing for over 200 round trips in the guide (Kim *et al.*, 2021).

It is interesting to note that an atom interferometer can be based on free propagation (Akatsuka *et al.*, 2017; Wang *et al.*, 2005) or fully-trapped atom clouds (clock type interferometers) (Navez *et al.*, 2016; Stevenson *et al.*, 2015) The first case can be pictured as the atoms functioning as an inertial reference much like a flywheel. The phase shift occurred by the fully trapped matter waves is maybe best understood as being based relativistic time gains of an atom clock (Hafele and Keating, 1972).

V. REMARKS AND FUTURE PERSPECTIVES

Atomtronics defines a new technology of micrometer-scale coherent networks to address both technology and basic science. It combines bottom-up and a top-down approaches: On one hand, the circuit elements can be designed to implement the microscopic theory in an experimental realization of unprecedented precision. Then, just like in electronics, different circuit elements can be assembled using a hierarchy of heuristic principles. On the other hand, a circuit or even a single circuital element in its own can be used as a current-based quantum simulator to probe the correlated matter.

Important domains of quantum many-body physics in restricted geometries, ranging from intermediate to extended spatial scales, now become accessible: Analogous to the analysis of current-voltage characteristics in solid state physics, atomtronic circuits have the potential to define current-based emulators and simulators, effectively widening the scope of the existing ones. Currents in particular are the natural quantity to explore not only superflows but also transport in disordered and complex media as well as topological properties and edge states. Another interesting direction to go is to exploit atomtronic circuits to address important questions of high energy physics, such as the phase diagram of quark-gluon plasma (Cazalilla *et al.*, 2009; He *et al.*, 2006; Ozawa and Baym, 2010; Rapp *et al.*, 2007) or various scattering process in elementary particles physics (Clark *et al.*, 2017; Fu *et al.*, 2020; Surace and Lerose, 2021). Bosonic rings can be employed to study the dynamics of the expanding universe (Eckel *et al.*, 2018).

Atomtronic circuitry has a practical potential as well — a potential that can be realized in part by leveraging the know-how and heuristic design principles of electronics. Atomtronic triple-well transistors are in many respects close analogs of their electronic field-effect transistor counterparts and can be utilized in matter wave oscillators, for example, to produce matter waves with high spatial coherence (Anderson, 2021), which in turn

can carry modulated signals or be used in sensing applications. In the future, one can expect many of the familiar elemental functions of electronic circuitry such as amplifiers, switches, oscillators, and so forth, to be carried over to the quantum regime.

Building on the theoretically demonstrated qubit dynamics of specific matter wave circuits (see Sect. IV.C), it will be certainly important to explore atomtronics as a platform for quantum gates. At the same time, matter-wave circuits provide a valuable route to realize high precision compact interferometers working on a wide range of sensitivity and very controllable physical conditions. Such devices are of considerable technological importance in different contexts ranging from inertial navigation (Bongs *et al.*, 2019) to geophysics (Jaroszewicz *et al.*, 2016). Unlike their classical or quantum electronic counterparts, atomtronic circuits can operate a regime in which quantum effects can be dominant and long coherence times are possible with a much simpler cryogenics. In this context, experimental, theoretical and technological inputs are envisaged to be combined together to realize the optimal building block circuit from which complex structures forming actual devices and sensors can be constructed. An important challenge to face in the years to come is to integrate the atomtronic circuits with other existing technologies such as photonic integrated circuits. Such hybrid networks may provide a valuable route for the fabrication of integrated 3D matter-wave circuits in which rectilinear, ring guides, beam splitters etc, together with the fields for the control and read-out of the quantum states and the lasers needed for cooling and manipulation of the cold atoms are built into a single chip. Such an approach can be important to achieve scalable matter-wave circuits.

Both for studies in fundamental science and circuit design with wider specifications, an interesting future direction is to expand the investigations to fermionic atomtronic circuits or to open the research in the field to new platforms, as e.g. fermionic systems with N spin components and Rydberg atoms. In such platforms, bath engineering can be explored to start the current beyond the current routes (Damanet *et al.*, 2019a,b; Keck *et al.*, 2018; Uchino and Brantut, 2020).

Acknowledgments

We thank G. Birk, P. Bouyer, C. Clark, J. Dalibard, R. Dumke, R. Folman, B. Garraway, T. Giannetti, T. Haug, T. Neely, S. Pandey, H. Perrin, J. Polo-Gomez, C. Sackett, and J. Schmiedmayer for comments and suggestions on the manuscript. We acknowledge fruitful discussions with J.I. Latorre, T. Leggett, C. Miniatura, P. Naldesi, G. Pecci, G. Roati, F. Scazza, K. Wright.

References

Abad, M., 2016, Phys. Rev. A **93**, 033603.

Abad, M., A. Sartori, S. Finazzi, and A. Recati, 2014, Phys. Rev. A **89**, 053602.

Affleck, I., 1988, Nuclear Physics B **305**(4), 582.

Aghamalyan, D., 2015, *Atomtronics: Quantum technology with cold atoms in ring shaped optical lattices*, Ph.D. thesis, National University of Singapore.

Aghamalyan, D., M. Cominotti, M. Rizzi, D. Rossini, F. Hekking, A. Minguzzi, L. C. Kwek, and L. Amico, 2015, New J. Phys. **17**(4), 045023.

Aghamalyan, D., N. Nguyen, F. Auksztol, K. Gan, M. M. Valado, P. Condylis, L. Kwek, R. Dumke, and L. Amico, 2016, New Journal of Physics **18**(7), 075013.

Aharonov, Y., and D. Bohm, 1959, Phys. Rev. **115**, 485.

Akatsuka, T., T. Takahashi, and H. Katori, 2017, Applied Physics Express **10**(11), 112501.

Albiez, M., R. Gati, J. Fölling, S. Hunsmann, M. Cristiani, and M. K. Oberthaler, 2005, Phys. Rev. Lett. **95**(1), 010402.

Amico, L., 2000, Modern Physics Letters B **14**(21), 759.

Amico, L., D. Aghamalyan, F. Auksztol, H. Crepaz, R. Dumke, and L. C. Kwek, 2014, Sci. Rep. **4**, 4298.

Amico, L., G. Birk, M. Boshier, and L.-C. Kwek, 2017, New Journal of Physics **19**(2), 020201.

Amico, L., M. Boshier, G. Birk, A. Minguzzi, C. Miniatura, L.-C. Kwek, D. Aghamalyan, V. Ahufinger, D. Anderson, N. Andrei, *et al.*, 2020, arXiv preprint arXiv:2008.04439 .

Amico, L., and V. Korepin, 2004, Annals of Physics **314**(2), 496.

Amico, L., A. Osterloh, and F. Cataliotti, 2005, Phys. Rev. Lett. **95**(6), 063201.

Amico, L., and V. Penna, 2000, Physical Review B **62**(2), 1224.

An, F. A., E. J. Meier, and B. Gadway, 2018, Phys. Rev. X **8**, 031045.

Anderson, D. Z., 2021, arXiv preprint arXiv:2106.10550 .

Andersson, E., T. Calarco, R. Folman, M. Andersson, B. Hessmo, and J. Schmiedmayer, 2002, Phys. Rev. Lett. **88**(10), 100401.

Andrei, N., 1995, Low-Dimensional Quantum Field Theories for Condensed Matter Physicists (World Scientific Publishing Co, 2013) pp , 457.

Andrews, M. R., C. G. Townsend, H.-J. Miesner, D. S. Durfee, D. M. Kurn, and W. Ketterle, 1997, Science **275**(5300), 637.

Anoshkin, K., Z. Wu, and E. Zaremba, 2013, Phys. Rev. A **88**, 013609.

Arabahmadi, E., D. Schumayer, and D. A. W. Hutchinson, 2021, Phys. Rev. A **103**, 043319.

Arimondo, E., W. Ertmer, W. Schleich, and E. Rasel, 2009, *Atom Optics and Space Physics: Proceedings of the International School of Physics “Enrico Fermi”, Course CLXVIII, Varenna on Lake Como, Villa Monastero, 3-13 July 2007*, volume 168 (IOS Press).

Arlt, J., T. Hitomi, and K. Dholakia, 2000, Applied Physics B **71**(4), 549.

Arnold, A. S., C. S. Garvie, and E. Riis, 2006, Physical Review A **73**(4), 041606.

Arnold, A. S., C. MacCormick, and M. G. Boshier, 2002, Phys. Rev. A **65**, 031601.

Aubin, S., S. Myrskog, M. Extavour, L. LeBlanc, D. McKay, A. Stummer, and J. Thywissen, 2006, Nature Physics **2**(6), 384.

Averin, D., and A. Bardas, 1995, Phys. Rev. Lett. **75**, 1831.

Baeriswyl, D., D. K. Campbell, J. M. Carmelo, F. Guinea,

and E. Louis, 2013, *The Hubbard model: its physics and mathematical physics*, volume 343 (Springer Science & Business Media).

Baiborodov, Y. T., M. S. Ioffe, V. M. Petrov, and R. I. Sobolev, 1963, Journal of Nuclear Energy. Part C **5**(6), 409.

Barontini, G., R. Labouvie, F. Stubenrauch, A. Vogler, V. Guarnera, and H. Ott, 2013, Phys. Rev. Lett. **110**, 035302.

Beattie, S., S. Moulder, R. J. Fletcher, and Z. Hadzibabic, 2013, Phys. Rev. Lett. **110**(2).

Bell, T. A., G. Gauthier, T. W. Neely, H. Rubinsztein-Dunlop, M. J. Davis, and M. A. Baker, 2018, Physical Review A **98**(1), 013604.

Bell, T. A., J. A. P. Glidden, L. Humbert, M. W. J. Bromley, S. A. Haine, M. J. Davis, T. W. Neely, M. A. Baker, and H. Rubinsztein-Dunlop, 2016, New Journal of Physics **18**(3), 035003.

Bentine, E., T. L. Harte, K. Luksch, A. J. Barker, J. Mur-Petit, B. Yuen, and C. J. Foot, 2017, Journal of Physics B **50**(9), 094002.

Bernon, S., H. Hattermann, D. Bothner, M. Knufinke, P. Weiss, F. Jessen, D. Cano, M. Kemmler, R. Kleiner, D. Koelle, *et al.*, 2013, Nature Communications **4**(1), 1.

Betz, T., S. Manz, R. Bücker, T. Berrada, C. Koller, G. Kazakov, I. E. Mazets, H.-P. Stimming, A. Perrin, T. Schumm, and J. Schmiedmayer, 2011, Phys. Rev. Lett. **106**, 020407.

Binanti, F., K. Furutani, and L. Salasnich, 2021, arXiv preprint arXiv:2104.11259 .

Birkl, G., F. Buchkremer, R. Dumke, and W. Ertmer, 2001, Optics Communications **191**(1-2), 67.

Bleszynski-Jayich, A., W. Shanks, B. Peaudecerf, E. Ginossar, F. Von Oppen, L. Glazman, and J. Harris, 2009, Science **326**(5950), 272.

Bloch, I., 2005, Nat. Phys. **1**(1), 23.

Bloch, I., J. Dalibard, and W. Zwerger, 2008, Rev. Mod. Phys. **80**(3), 885.

Boada, O., A. Celi, J. I. Latorre, and M. Lewenstein, 2012, Phys. Rev. Lett. **108**, 133001.

Bongs, K., S. Burger, S. Dettmer, D. Hellweg, J. Arlt, W. Ertmer, and K. Sengstock, 2001, Physical Review A - Atomic, Molecular, and Optical Physics **63**, 031602(R).

Bongs, K., M. Holynski, J. Vovrosh, P. Bouyer, G. Condon, E. Rasel, C. Schubert, W. P. Schleich, and A. Roura, 2019, Nature Reviews Physics **1**(12), 731.

Boyer, V., C. M. Chandrashekhar, C. J. Foot, and Z. J. Laczik, 2004, Journal of Modern Optics **51**(14), 2235.

Boyer, V., R. M. Godun, G. Smirne, D. Cassetta, C. M. Chandrashekhar, A. B. Deb, Z. J. Laczik, and C. J. Foot, 2006, Physical Review A (Atomic, Molecular, and Optical Physics) **73**(3), 031402.

Brantut, J.-P., C. Grenier, J. Meineke, D. Stadler, S. Krinner, C. Kollath, T. Esslinger, and A. Georges, 2013, Science **342**(6159), 713.

Brantut, J.-P., J. Meineke, D. Stadler, S. Krinner, and T. Esslinger, 2012, Science **337**(6098), 1069.

Breuer, H.-P., and F. Petruccione, 2002, *The theory of open quantum systems* (Oxford University Press on Demand).

Bruderer, M., and W. Belzig, 2012, Phys. Rev. A **85**, 013623.

Bulut, I., and F. Nori, 2009, Science **326**(5949), 108.

Burchianti, A., F. Scazza, A. Amico, G. Valtolina, J. A. Seman, C. Fort, M. Zaccanti, M. Inguscio, and G. Roati, 2018, Phys. Rev. Lett. **120**, 025302.

Burke, J. H. T., B. Deissler, K. J. Hughes, and C. A. Sackett, 2008, Physical Review A **78**(2).

Burke, J. H. T., and C. A. Sackett, 2009, Physical Review A **80**, 061603.

Buser, M., C. Hubig, U. Schollwöck, L. Tarruell, and F. Heidrich-Meisner, 2020, Physical Review A **102**(5), 053314.

Büttiker, M., Y. Imry, and M. Y. Azbel, 1984, Phys. Rev. A **30**(4), 1982.

Büttiker, M., Y. Imry, and R. Landauer, 1983, Physics Letters A **96**(7), 365.

Byers, N., and C. Yang, 1961, Phys. Rev. Lett. **7**(2), 46.

Cai, Y., D. G. Allman, P. Sabharwal, and K. C. Wright, 2021, arXiv preprint arXiv:2104.02218 .

Caliga, S. C., C. J. Straatsma, and D. Z. Anderson, 2016a, New Journal of Physics **18**(2), 025010.

Caliga, S. C., C. J. Straatsma, and D. Z. Anderson, 2017, New Journal of Physics **19**(1), 013036.

Caliga, S. C., C. J. Straatsma, A. A. Zozulya, and D. Z. Anderson, 2016b, New Journal of Physics **18**(1), 015012.

Caliga, S. C., C. J. E. Straatsma, A. A. Zozulya, and D. Z. Anderson, 2012, arXiv preprint arXiv:1208.3109 .

Calogero, F., and A. Degasperis, 1975, Phys. Rev. A **11**, 265.

Cano, D., B. Kasch, H. Hattermann, R. Kleiner, C. Zimmermann, D. Koelle, and J. Fortágh, 2008, Phys. Rev. Lett. **101**, 183006.

Cappellini, G., M. Mancini, G. Pagano, P. Lombardi, L. Livi, M. S. de Cumis, P. Cancio, M. Pizzocaro, D. Calonico, F. Levi, *et al.*, 2014, Phys. Rev. Lett. **113**(12), 120402.

Capponi, S., P. Lecheminant, and K. Totsuka, 2016, Annals of Physics **367**, 50.

Cassettari, D., B. Hessmo, R. Folman, T. Maier, and J. Schmiedmayer, 2000, Physical Review Letters **85**(26), 5483, ISSN 0031-9007.

Cazalilla, M. A., R. Citro, T. Giamarchi, E. Orignac, and M. Rigol, 2011, Rev. Mod. Phys. **83**, 1405, URL <https://link.aps.org/doi/10.1103/RevModPhys.83.1405>.

Cazalilla, M. A., A. Ho, and M. Ueda, 2009, New Journal of Physics **11**(10), 103033.

Cazalilla, M. A., and A. M. Rey, 2014, Reports on Progress in Physics **77**(12), 124401.

Celi, A., P. Massignan, J. Ruseckas, N. Goldman, I. B. Spielman, G. Juzeliūnas, and M. Lewenstein, 2014, Phys. Rev. Lett. **112**, 043001.

Chakraborty, T., and P. Pietiläinen, 1994, Physical Review B **50**(12), 8460.

Chetcuti, W. J., T. Haug, L.-C. Kwek, and L. Amico, 2020, arXiv preprint arXiv:2011.00916 .

Chien, C.-C., M. Di Ventra, and M. Zwolak, 2014, Phys. Rev. A **90**, 023624.

Choy, T., and F. Haldane, 1982, Physics Letters A **90**(1-2), 83.

Cirac, J. I., and P. Zoller, 2012, Nat Phys **8**(4), 264.

Clark, L. W., A. Gaj, L. Feng, and C. Chin, 2017, Nature **551**(7680), 356.

Cohen-Tannoudji, C., and S. Reynaud, 1977, Journal of Physics B: Atomic and Molecular Physics **10**(3), 345.

Colombe, Y., E. Knyazchyan, O. Morizot, B. Mercier, V. Lorent, and H. Perrin, 2004, Europhysics Letters **46**7, 593.

Cominotti, M., M. Rizzi, D. Rossini, D. Aghamalyan, L. Amico, L. C. Kwek, F. Hekking, and A. Minguzzi, 2015, The European Physical Journal Special Topics **224**(3), 519.

Cominotti, M., D. Rossini, M. Rizzi, F. Hekking, and A. Minguzzi, 2014, Phys. Rev. Lett. **113**(2), 025301.

Corman, L., L. Chomaz, T. Bienaimé, R. Desbuquois, C. Weitenberg, S. Nascimbene, J. Dalibard, and J. Beugnon, 2014, Phys. Rev. Lett. **113**(13), 135302.

Corman, L., P. Fabritius, S. Häusler, J. Mohan, L. H. Dogra, D. Husmann, M. Lebrat, and T. Esslinger, 2019, Phys. Rev. A **100**, 053605.

Cornell, E. A., and C. E. Wieman, 2002, Reviews of Modern Physics **74**(3), 875.

Couvert, A. Couvert, M. Jeppesen, T. Kawalec, G. Reinaudi, R. Mathevet, and D. Guéry-Odelin, 2008, EPL **83**(5), 6 pages.

Crompvoets, F. M., H. L. Bethlehem, R. T. Jongma, and G. Meijer, 2001, Nature **411**(6834), 174.

Cronin, A. D., J. Schmiedmayer, and D. E. Pritchard, 2009, Reviews of Modern Physics **81**(3), 1051.

Cuevas, J. C., and E. Scheer, 2017, *Molecular Electronics*, volume Volume 15 (World Scientific).

Curtis, J. E., B. A. Koss, and D. G. Grier, 2002, Optics Communications **207**(1), 169.

Daley, A., P. Zoller, and B. Trauzettel, 2008, Phys. Rev. Lett. **100**(11), 110404.

Dalfovo, F., S. Giorgini, L. P. Pitaevskii, and S. Stringari, 1999, Rev. Mod. Phys. **71**(3), 463.

Dalibard, J., F. Gerbier, G. Juzeliūnas, and P. Öhberg, 2011, Rev. Mod. Phys. **83**(4), 1523.

Dall, R. G., S. S. Hodgman, M. T. Johnsson, K. G. H. Baldwin, and A. G. Truscott, 2010, Physical Review A **81**(1), 011602.

Damanet, F., E. Mascarenhas, D. Pekker, and A. J. Daley, 2019a, Phys. Rev. Lett. **123**, 180402.

Damanet, F., E. Mascarenhas, D. Pekker, and A. J. Daley, 2019b, New Journal of Physics **21**(11), 115001.

Danshita, I., and A. Polkovnikov, 2012, Phys. Rev. A **85**, 023638.

David, T., Y. Japha, V. Dikovsky, R. Salem, C. Henkel, and R. Folman, 2008, The European Physical Journal D **48**(3), 321.

Davis, T. J., 1999, Journal of Optics B: **1**(4), 408.

Deaver, B. S., and W. M. Fairbank, 1961, Phys. Rev. Lett. **7**, 43.

Degen, C. L., F. Reinhard, and P. Cappellaro, 2017, Rev. Mod. Phys. **89**(3), 035002.

Deissler, B., K. Hughes, J. Burke, and C. Sackett, 2008, Physical Review A **77**(3), 031604.

Del Pace, G., W. J. Kwon, M. Zaccanti, G. Roati, and F. Scazza, 2021, Phys. Rev. Lett. **126**, 055301.

Denschlag, J., D. Cassettari, A. Chenet, S. Schneider, and J. Schmiedmayer, 1999a, Applied Physics B **69**(4), 291.

Denschlag, J., D. Cassettari, and J. Schmiedmayer, 1999b, Physical Review Letters **82**(10), 2014.

Dikovsky, V., Y. Japha, C. Henkel, and R. Folman, 2005, The European Physical Journal D-Atomic, Molecular, Optical and Plasma Physics **35**(1), 87.

Dikovsky, V., V. Sokolovsky, B. Zhang, C. Henkel, and R. Folman, 2009, The European Physical Journal D **51**(2), 247.

Diot, D., Y.-J. Wang, D. Anderson, E. Cornell, R. Saravanan, V. Bright, and M. Prentiss, 2004, International Quantum Electronics Conference, 2004. (IQEC). , 60.

Dowling, J. P., and G. J. Milburn, 2003, Philosophical Transactions of the Royal Society of London A: Mathematical, Physical and Engineering Sciences **361**(1809), 1655.

Dubessy, R., T. Liennard, P. Pedri, and H. Perrin, 2012, Phys. Rev. A **86**, 011602.

Dubessy, R., J. Polo, H. Perrin, A. Minguzzi, and M. Olshanii, 2021, Phys. Rev. Research **3**, 013098.

Dumke, R., T. Müther, M. Volk, W. Ertmer, and G. Birk, 2002, Physical Review Letters **89**(22), 220402.

Dutta, O., M. Gajda, P. Hauke, M. Lewenstein, D.-S. Lühmann, B. A. Malomed, T. Sowiński, and J. Zakrzewski, 2015, Reports on Progress in Physics **78**(6), 066001.

Eckel, S., F. Jendrzejewski, A. Kumar, C. J. Lobb, and G. K. Campbell, 2014a, Phys. Rev. X **4**(3), 031052.

Eckel, S., A. Kumar, T. Jacobson, I. B. Spielman, and G. K. Campbell, 2018, Phys. Rev. X **8**, 021021.

Eckel, S., J. G. Lee, F. Jendrzejewski, C. J. Lobb, G. K. Campbell, and W. T. Hill, 2016, Phys. Rev. A **93**, 063619.

Eckel, S., J. G. Lee, F. Jendrzejewski, N. Murray, C. W. Clark, C. J. Lobb, W. D. Phillips, M. Edwards, and G. K. Campbell, 2014b, Nature **506**(7487), 200–203.

Essler, F. H., H. Frahm, F. Göhmann, A. Klümper, and V. E. Korepin, 2005, *The one-dimensional Hubbard model* (Cambridge University Press).

Fabre, C. M., P. Cheiney, G. L. Gattobigio, F. Vermersch, S. Faure, R. Mathevet, T. Lahaye, and D. Guéry-Odelin, 2011, Physical Review Letters **107**(23), 230401.

Faddeev, L., and L. Takhtajan, 2007, *Hamiltonian methods in the theory of solitons* (Springer Science & Business Media).

Fazio, R., and H. Van Der Zant, 2001, Physics Reports **355**(4), 235.

Fernholz, T., R. Gerritsma, S. Whitlock, I. Barb, and R. J. C. Spreeuw, 2008, Physical Review A **77**(3).

Filippone, M., F. Hekking, and A. Minguzzi, 2016, Phys. Rev. A **93**, 011602.

Fisher, M. P., P. B. Weichman, G. Grinstein, and D. S. Fisher, 1989, Physical Review B **40**(1), 546.

Fleischhauer, M., A. Imamoglu, and J. P. Marangos, 2005, Reviews of modern physics **77**(2), 633.

Folman, R., P. Krüger, D. Cassettari, B. Hessmo, T. Maier, and J. Schmiedmayer, 2000, Physical Review Letters **84**(20), 4749.

Folman, R., P. Krüger, J. Schmiedmayer, J. Denschlag, and C. Henkel, 2008, arXiv preprint arXiv:0805.2613 .

Fortágh, J., and C. Zimmermann, 2007, Reviews of Modern Physics **79**(1), 235.

Franke-Arnold, S., J. Leach, M. Padgett, V. Lembessis, D. Ellinas, A. Wright, J. Girkin, P. Ohberg, and A. Arnold, 2007, Optics Express **15**(14), 8619.

Friedman, N., A. Kaplan, D. Carasso, and N. Davidson, 2001, Physical Review Letters **86**(8), 1518.

Frye, K., S. Abend, W. Bartosch, A. Bawamia, D. Becker, H. Blume, C. Braxmaier, S.-W. Chiow, M. A. Efremov, W. Ertmer, P. Fierlinger, T. Franz, *et al.*, 2021, EPJ Quantum Technology **8**(1), 1.

Fu, H., Z. Zhang, K.-X. Yao, L. Feng, J. Yoo, L. W. Clark, K. Levin, and C. Chin, 2020, Physical Review Letters **125**(18), 183003.

Gallego-Marcos, F., G. Platero, C. Nietner, G. Schaller, and T. Brandes, 2014, Phys. Rev. A **90**, 033614.

Gallemí, A., M. Guilleumas, M. Richard, and A. Minguzzi, 2018, Phys. Rev. B **98**, 104502.

Garcia, O., B. Deissler, K. J. Hughes, J. M. Reeves, and C. A. Sackett, 2006, Physical Review A **74**(3), 031601.

Garraway, B. M., and H. Perrin, 2016, Journal of Physics B **49**(17), 172001.

Gati, R., B. Hemmerling, J. Fölling, M. Albiz, and M. K. Oberthaler, 2006, Physical Review Letters **96**(13), 130404.

Gattobigio, G. L., A. Couvert, G. Reinaudi, B. Georgeot, and

D. Guéry-Odelin, 2012, Physical Review Letters **109**(3), 030403.

Gaunt, A. L., and Z. Hadzibabic, 2012, Scientific Reports **2**, 721.

Gauthier, G., T. A. Bell, A. B. Stilgoe, M. Baker, H. Rubinsztein-Dunlop, and T. W. Neely, 2021, arXiv preprint arXiv:2103.10020 .

Gauthier, G., I. Lenton, N. M. Parry, M. Baker, M. Davis, H. Rubinsztein-Dunlop, and T. Neely, 2016, Optica **3**(10), 1136.

Gauthier, G., S. S. Szigeti, M. T. Reeves, M. Baker, T. A. Bell, H. Rubinsztein-Dunlop, M. J. Davis, and T. W. Neely, 2019, Phys. Rev. Lett. **123**, 260402.

Gefen, Y., Y. Imry, and M. Y. Azbel, 1984, Phys. Rev. Lett. **52**(2), 129.

Gehr, R., J. Volz, G. Dubois, T. Steinmetz, Y. Colombe, B. L. Lev, R. Long, J. Esteve, and J. Reichel, 2010, Phys. Rev. Lett. **104**(20), 203602.

Geiger, R., A. Landragin, S. Merlet, and F. Pereira Dos Santos, 2020, AVS Quantum Science **2**(2), 024702.

Geiger, R., V. Ménoret, G. Stern, N. Zahzam, P. Cheinet, B. Battelier, A. Villing, F. Moron, M. Lours, Y. Bidel, *et al.*, 2011, Nature communications **2**(1), 1.

Giamarchi, T., 2003, *Quantum Physics in One Dimension*, International Series of Monographs on Physics (Clarendon Press).

Giovannazzi, S., J. Esteve, and M. K. Oberthaler, 2008, **10**(4), 045009.

Goldman, N., G. Juzeliūnas, P. Öhberg, and I. B. Spielman, 2014, Reports on Progress in Physics **77**(12), 126401.

Grenier, C., A. Georges, and C. Kollath, 2014, Phys. Rev. Lett. **113**, 200601.

Grenier, C., C. Kollath, and A. Georges, 2016, Comptes Rendus Physique **17**, 1161.

Grimm, R., M. Weidemüller, and Y. B. Ovchinnikov, 2000, *Optical Dipole Traps for Neutral Atoms* (Academic Press), volume 42, pp. 95–170.

Gring, M., M. Kuhnert, T. Langen, T. Kitagawa, B. Rauer, M. Schreitl, I. Mazets, D. A. Smith, E. Demler, and J. Schmiedmayer, 2012, Science **337**(6100), 1318.

Gritsev, V., A. Polkovnikov, and E. Demler, 2007, Phys. Rev. B **75**, 174511.

Guan, X.-W., M. T. Batchelor, and C. Lee, 2013, Reviews of Modern Physics **85**(4), 1633.

Guarrera, V., R. Moore, A. Bunting, T. Vanderbruggen, and Y. B. Ovchinnikov, 2017, Scientific Reports **7**(1), 4749.

Guerin, W., J.-F. Riou, J. P. Gaebler, V. Josse, P. Bouyer, and A. Aspect, 2006, Phys. Rev. Lett. **97**, 200402.

Guo, Y., R. Dubessy, M. d. G. de Herve, A. Kumar, T. Badr, A. Perrin, L. Longchambon, and H. Perrin, 2020, Phys. Rev. Lett. **124**(2), 025301.

Gupta, S., K. Murch, K. Moore, T. Purdy, and D. Stamper-Kurn, 2005, Phys. Rev. Lett. **95**(14), 143201.

Gustavson, T. L., P. Bouyer, and M. A. Kasevich, 1997, Phys. Rev. Lett. **78**, 2046.

Gustavson, T. L., A. Landragin, and M. A. Kasevich, 2000, Classical and Quantum Gravity **17**(12), 2385.

Gutiérrez-Medina, B., 2013, American Journal of Physics **81**(2), 104, ISSN 0002-9505.

Gutman, D. B., Y. Gefen, and A. D. Mirlin, 2012, Phys. Rev. B **85**, 125102.

Gutzwiller, M. C., 1963, Phys. Rev. Lett. **10**(5), 159.

Ha, L.-C., L. W. Clark, C. V. Parker, B. M. Anderson, and C. Chin, 2015, Phys. Rev. Lett. **114**, 055301.

Hafele, J. C., and R. E. Keating, 1972, Science **177**(4044), 168.

Haine, S. A., 2018, New Journal of Physics **20**(3), 033009.

Haldane, F., 1980, Physics Letters A **80**(4), 281.

Halkyard, P. L., M. P. A. Jones, and S. A. Gardiner, 2010, Physical Review A **81**(6), .

Hallwood, D. W., K. Burnett, and J. Dunningham, 2006, New Journal of Physics **8**(9), 180.

Hallwood, D. W., K. Burnett, and J. Dunningham, 2007, Journal of Modern Optics **54**(13-15), 2129.

Hallwood, D. W., T. Ernst, and J. Brand, 2010, Physical Review A **82**(6), 063623.

Hammerer, K., A. S. Sørensen, and E. S. Polzik, 2010, Reviews of Modern Physics **82**(2), 1041.

Hänsel, W., P. Hommelhoff, T. Hänsch, and J. Reichel, 2001, Nature **413**(6855), 498.

Harber, D., J. Obrecht, J. McGuirk, and E. Cornell, 2005, Physical Review A **72**(3), 33610.

Haroche, S., and J.-M. Raimond, 2006, *Exploring the quantum: atoms, cavities, and photons* (Oxford University Press).

Hattermann, H., D. Bothner, L. Ley, B. Ferdinand, D. Wiedmaier, L. Sárkány, R. Kleiner, D. Koelle, and J. Fortágh, 2017, Nature communications **8**(1), 1.

Haug, T., L. Amico, R. Dumke, and L.-C. Kwek, 2018a, Quantum Science and Technology **3**(3), 035006.

Haug, T., R. Dumke, L.-C. Kwek, and L. Amico, 2019a, Quantum Sci. Technol. **4**(4), 045001.

Haug, T., R. Dumke, L.-C. Kwek, and L. Amico, 2019b, Commun. Phys. **2**(1), 1.

Haug, T., R. Dumke, L.-C. Kwek, C. Miniatura, and L. Amico, 2021, Phys. Rev. Research **3**, 013034.

Haug, T., H. Heimonen, R. Dumke, L.-C. Kwek, and L. Amico, 2019c, Physical Review A **100**(4), 041601.

Haug, T., J. Tan, M. Theng, R. Dumke, L.-C. Kwek, and L. Amico, 2018b, Phys. Rev. A **97**(1), 013633.

Haug, T. F., 2020, *Quantum transport with cold atoms*, Ph.D. thesis, National University of Singapore, URL <https://scholarbank.nus.edu.sg/handle/10635/190520>.

Häusler, S., S. Nakajima, M. Lebrat, D. Husmann, S. Krinner, T. Esslinger, and J.-P. Brantut, 2017, Phys. Rev. Lett. **119**, 030403.

He, L., M. Jin, and P. Zhuang, 2006, Physical Review A **74**(3), 033604.

Hekking, F., and L. Glazman, 1997, Physical Review B **55**(10), 6551.

Helm, J., S. Cornish, and S. Gardiner, 2015, Phys. Rev. Lett. **114**(13), 134101.

Helm, J., S. Rooney, C. Weiss, and S. Gardiner, 2014, Physical Review A **89**(3), 033610.

Helm, J. L., T. P. Billam, and S. A. Gardiner, 2012, Phys. Rev. A **85**, 053621.

Helm, J. L., T. P. Billam, A. Rakonjac, S. L. Cornish, and S. A. Gardiner, 2018, Physical Review Letters **120**(6), 063201.

Henderson, K., C. Ryu, C. MacCormick, and M. G. Boshier, 2009, New Journal of Physics **11**(4), 043030.

Hod, O., R. Baer, and E. Rabani, 2006, Phys. Rev. Lett. **97**(26), 266803.

Hofferberth, S., I. Lesanovsky, B. Fischer, T. Schumm, and J. Schmiedmayer, 2007, Nature **449**(7160), 324.

Hofferberth, S., I. Lesanovsky, B. Fischer, J. Verdu, and J. Schmiedmayer, 2006, Nature Physics **2**(10), 710, ISSN 1745-2473.

Hofferberth, S., I. Lesanovsky, T. Schumm, A. Imambeikov, V. Gritsev, E. Demler, and J. Schmiedmayer, 2008, *Nature Physics* **4**(6), 489.

Houde, O., D. Kadio, and L. Pruvost, 2000, *Physical Review Letters* **85**(26), 5543.

Hubbard, J., 1963, *Proceedings of the Royal Society of London. Series A. Mathematical and Physical Sciences* **276**(1365), 238.

Hueck, K., A. Mazurenko, N. Luick, T. Lompe, and H. Moritz, 2017, *Review of Scientific Instruments* **88**(1), 016103.

Husmann, D., M. Lebrat, S. Häusler, J.-P. Brantut, L. Corman, and T. Esslinger, 2018, *Proceedings of the National Academy of Sciences* .

Husmann, D., S. Uchino, S. Krinner, M. Lebrat, T. Giamarchi, T. Esslinger, and J.-P. Brantut, 2015, *Science* **350**(6267), 1498.

Imry, Y., 2002, *Introduction to mesoscopic physics* (Oxford University Press).

Imry, Y., and R. Landauer, 1999, *Rev. Mod. Phys.* **71**, S306.

Ivanov, A., G. Kordas, A. Komnik, and S. Wimberger, 2013, *The European Physical Journal B* **86**(8), 345.

Jagla, E., and C. Balseiro, 1993, *Phys. Rev. Lett.* **70**(5), 639.

Jaksch, D., C. Bruder, J. I. Cirac, C. W. Gardiner, and P. Zoller, 1998, *Phys. Rev. Lett.* **81**(15), 3108.

Japha, Y., O. Arzouan, Y. Avishai, and R. Folman, 2007, *Physical Review Letters* **99**(6), 060402.

Jaroszewicz, L. R., A. Kurzych, Z. Krajewski, P. Marć, J. K. Kowalski, P. Bobra, Z. Zembaty, B. Sakowicz, and R. Jankowski, 2016, *Sensors* **16**(12), 2161.

Jendrzejewski, F., S. Eckel, N. Murray, C. Lanier, M. Edwards, C. J. Lobb, and G. K. Campbell, 2014, *Phys. Rev. Lett.* **113**(4), 045305.

Jones, M. P. A., C. J. Vale, D. Sahagun, B. V. Hall, C. C. Eberlein, B. Sauer, K. Furusawa, D. Richardson, and E. A. Hinds, 2004, *Journal of Physics B* **37**(2), L15.

Jördens, R., N. Strohmaier, K. Günter, H. Moritz, and T. Esslinger, 2008, *Nature* **455**(7210), 204.

Kanamori, J., 1963, *Progress of Theoretical Physics* **30**(3), 275.

Kanász-Nagy, M., L. Glazman, T. Esslinger, and E. A. Demler, 2016, *Phys. Rev. Lett.* **117**, 255302.

Kasch, B., H. Hattermann, D. Cano, T. Judd, S. Scheel, C. Zimmermann, R. Kleiner, D. Koelle, and J. Fortágh, 2010, *New Journal of Physics* **12**(6), 065024.

Keck, M., D. Rossini, and R. Fazio, 2018, *Physical Review A* **98**(5), 053812.

Keil, M., O. Amit, S. Zhou, D. Groswasser, Y. Japha, and R. Folman, 2016, *Journal of modern optics* **63**(18), 1840.

Ketterle, W., 2002, *Reviews of Modern Physics* **74**(4), 1131.

Khondker, A., M. R. Khan, and A. Anwar, 1988, *Journal of applied physics* **63**(10), 5191.

Kim, H., K. A. Krzyzanowska, K. C. Henderson, C. Ryu, E. M. C. Timmermans, and M. G. Boshier, 2021, *arXiv preprint arXiv:21XX.XXXX* .

Kim, S. J., H. Yu, S. T. Gang, and J. B. Kim, 2017, *Applied Physics B* **123**(5), 154, ISSN 0946-2171.

Kolovsky, A. R., 2017, *Phys. Rev. A* **96**, 011601.

Kolovsky, A. R., Z. Denis, and S. Wimberger, 2018, *Phys. Rev. A* **98**, 043623.

Korepin, V. E., N. M. Bogoliubov, and A. G. Izergin, 1997, *Quantum inverse scattering method and correlation functions*, volume 3 (Cambridge university press).

Kovachy, T., J. M. Hogan, A. Sugarbaker, S. M. Dickerson, C. A. Donnelly, C. Overstreet, and M. A. Kasevich, 2015, *Phys. Rev. Lett.* **114**, 143004.

Kraft, S., A. Günther, H. Ott, D. Wharam, C. Zimmermann, and J. Fortágh, 2002, *Journal of Physics B: Atomic, Molecular and Optical Physics* **35**(21), L469.

Kreutzmann, H., U. V. Poulsen, M. Lewenstein, R. Dumke, W. Ertmer, G. Birkl, and A. Sanpera, 2004, *Phys. Rev. Lett.* **92**(16).

Krinner, S., T. Esslinger, and J.-P. Brantut, 2017, *Journal of Physics: Condensed Matter* **29**(34), 343003.

Krinner, S., M. Lebrat, D. Husmann, C. Grenier, J.-P. Brantut, and T. Esslinger, 2016, *Proc. Nat. Acad. Sci.* **113**(29), 8144.

Krinner, S., D. Stadler, D. Husmann, J.-P. Brantut, and T. Esslinger, 2015a, *Nature* **517**(7532), 64.

Krinner, S., D. Stadler, J. Meineke, J.-P. Brantut, and T. Esslinger, 2013, *Phys. Rev. Lett.* **110**, 100601.

Krinner, S., D. Stadler, J. Meineke, J.-P. Brantut, and T. Esslinger, 2015b, *Phys. Rev. Lett.* **115**, 045302.

Krzyzanowska, K., J. Ferreras, C. Ryu, and M. Boshier, 2021, *arXiv preprint arXiv:21XX.XXXX* .

Krüger, P., L. M. Andersson, S. Wildermuth, S. Hofferberth, E. Haller, S. Aigner, S. Groth, I. Bar-Joseph, and J. Schmiedmayer, 2007, *Physical Review A* **76**(6), URL <https://doi.org/10.1103/physreva.76.063621>.

Kuga, T., Y. Torii, N. Shiokawa, T. Hirano, Y. Shimizu, and H. Sasada, 1997, *Physical Review Letters* **78**(25), 4713.

Kumar, A., N. Anderson, W. D. Phillips, S. Eckel, G. K. Campbell, and S. Stringari, 2016a, *New Journal of Physics* **18**(2), 025001, URL <https://doi.org/10.1088/1367-2630/18/2/025001>.

Kumar, A., N. Anderson, W. D. Phillips, S. Eckel, G. K. Campbell, and S. Stringari, 2016b, *New Journal of Physics* **18**(2), 025001, URL <https://doi.org/10.1088/1367-2630/18/2/025001>.

Kumar, A., S. Eckel, F. Jendrzejewski, and G. K. Campbell, 2017, *Phys. Rev. A* **95**(2), 021602.

Kunimi, M., and I. Danshita, 2017, *Phys. Rev. A* **95**, 033637.

Kwon, W. J., G. Del Pace, R. Panza, M. Inguscio, W. Zwinger, M. Zaccanti, F. Scazza, and G. Roati, 2020, *Science* **369**(6499), 84.

Labouvie, R., B. Santra, S. Heun, S. Wimberger, and H. Ott, 2015, *Phys. Rev. Lett.* **115**, 050601.

Lacki, M., M. Baranov, H. Pichler, Y. Wang, S. Subhankar, P. Bienias, T. Tsui, J. Porto, S. Rolston, A. Gorshkov, *et al.*, ????

Lamata, L., A. Mezzacapo, J. Casanova, E. Solano, T. H. Johnson, S. R. Clark, D. Jaksch, K. V. Krutitsky, P. Navez, F. Queisser, *et al.*, 2014, *Quantum* **1**(1).

Langen, T., R. Geiger, and J. Schmiedmayer, 2015, *Annual Review of Condensed Matter Physics* **6**(1), 201.

Leanhardt, A., A. Chikkatur, D. Kielpinski, Y. Shin, T. Gustavson, W. Ketterle, and D. Pritchard, 2002, *Phys. Rev. Lett.* **89**(4), 040401.

LeBlanc, L. J., A. B. Bardon, J. McKeever, M. H. T. Extavour, D. Jervis, J. H. Thywissen, F. Piazza, and A. Smerzi, 2011, *Phys. Rev. Lett.* **106**, 025302.

Lebrat, M., S. Häusler, P. Fabritius, D. Husmann, L. Corman, and T. Esslinger, 2019, *Phys. Rev. Lett.* **123**, 193605.

Lebrat, M., P. Grišins, D. Husmann, S. Häusler, L. Corman, T. Giamarchi, J.-P. Brantut, and T. Esslinger, 2018, *Phys. Rev. X* **8**, 011053.

Lee, T. D., K. Huang, and C. N. Yang, 1957, *Phys. Rev.* **106**, 1135.

Leggett, A., 2006, *Quantum Fluids* (Oxford University Press

Oxford).

Leggett, A. J., 1980, *Progr. Theoret. Phys. Suppl.* **69**, 80.

Leggett, A. J., 1991, *NATO ASI Ser. B* **251**, 297.

Lesanovsky, I., and W. von Klitzing, 2007, *Phys. Rev. Lett.* **99**(8), 083001.

Lévy, L. P., G. Dolan, J. Dunsmuir, and H. Bouchiat, 1990, *Phys. Rev. Lett.* **64**, 2074.

Levy, S., E. Lahoud, I. Shomroni, and J. Steinhauer, 2007, *Nature* **449**(7162), 579.

Lewenstein, M., A. Sanpera, and V. Ahufinger, 2012, *Ultra-cold Atoms in Optical Lattices: Simulating quantum many-body systems* (Oxford University Press).

Li, G., M. D. Fraser, A. Yakimenko, and E. A. Ostrovskaya, 2015, *Physical Review B* **91**(18), 184518.

Lieb, E. H., and W. Liniger, 1963, *Physical Review* **130**(4), 1605.

Lieb, E. H., and F. Wu, 1968, *Phys. Rev. Lett.* **21**(3), 192.

Lim, Y., J. Goo, H. Kwak, and Y. Shin, 2021, *Physical Review A* **103**(6), 063319.

Liu, B., H. Zhai, and S. Zhang, 2017, *Phys. Rev. A* **95**, 013623.

Lobos, A., and A. Aligia, 2008, *Phys. Rev. Lett.* **100**(1), 016803.

Long, R., T. Rom, W. Hansel, T. W. Hansch, and J. Reichel, 2005, *European Physical Journal D* **35**, 125.

Loss, D., 1992, *Phys. Rev. Lett.* **69**(2), 343.

Luick, N., L. Sobirey, M. Bohlen, V. P. Singh, L. Mathey, T. Lompe, and H. Moritz, 2020, *Science* **369**(6499), 89.

Lukoshkin, V. A., V. K. Kalevich, M. M. Afaniasiev, K. V. Kavokin, Z. Hatzopoulos, P. G. Savvidis, E. S. Sedov, and A. V. Kavokin, 2018, *Phys. Rev. B* **97**, 195149.

Mahan, G. D., 2013, *Many-particle physics* (Springer Science & Business Media).

Majorana, E., 1932, *Il Nuovo Cimento* **9**, 43.

Manmana, S. R., K. R. Hazzard, G. Chen, A. E. Feiguin, and A. M. Rey, 2011, *Physical Review A* **84**(4), 043601.

Marchukov, O., M. Olshanii, and B. Malomed, 2018, A model of splitting an nls breather by an emerging localized linear or nonlinear potential.

Marino, I., S. Raghavan, S. Fantoni, S. R. Shenoy, and A. Smerzi, 1999, *Phys. Rev. A* **60**, 487.

Marquardt, F., and C. Bruder, 2002, *Phys. Rev. B* **65**(12), 125315.

Mas, H., S. Pandey, G. Vasilakis, and W. von Klitzing, 2019, *New Journal of Physics* **21**, 123039.

Mathew, R., A. Kumar, S. Eckel, F. Jendrzejewski, G. K. Campbell, M. Edwards, and E. Tiesinga, 2015, *Phys. Rev. A* **92**, 033602.

Mathey, A. C., C. W. Clark, and L. Mathey, 2014, *Phys. Rev. A* **90**(2), 023604.

Matveev, K., A. Larkin, and L. Glazman, 2002, *Phys. Rev. Lett.* **89**(9), 096802.

McDonald, G. D., H. Keal, P. A. Altin, J. E. Debs, S. Bennetts, C. C. N. Kuhn, K. S. Hardman, M. T. Johnsson, J. D. Close, and N. P. Robins, 2013a, *Physical Review A* **87**(1), 013632.

McDonald, G. D., C. C. Kuhn, K. S. Hardman, S. Bennetts, P. J. Everitt, P. A. Altin, J. E. Debs, J. D. Close, and N. P. Robins, 2014, *Phys. Rev. Lett.* **113**(1), 013002.

McDonald, G. D., C. C. N. Kuhn, S. Bennetts, J. E. Debs, K. S. Hardman, M. Johnsson, J. D. Close, and N. P. Robins, 2013b, *Physical Review A* **88**(5), 053620.

McGloin, D., G. C. Spalding, H. Melville, W. Sibbett, and K. Dholakia, 2003, *Opt. Express* **11**(2), 158.

Meek, S. A., H. L. Bethlem, H. Conrad, and G. Meijer, 2008, *Phys. Rev. Lett.* **100**(15), 153003.

Meek, S. A., H. Conrad, and G. Meijer, 2009, *Science* **324**(5935), 1699.

Meier, F., and W. Zwerger, 2001, *Phys. Rev. A* **64**, 033610.

Mielke, A., 2015, *Many Body Physics: From Kondo to Hubbard. Modeling and Simulation* **5**.

Milburn, G., J. Corney, E. M. Wright, and D. Walls, 1997, *Physical Review A* **55**(6), 4318.

Milner, V., J. L. Hanssen, W. C. Campbell, and M. G. Raizen, 2001, *Physical Review Letters* **86**(8), 1514.

Moan, E. R., R. A. Horne, T. Arporntip, Z. Luo, A. J. Fallon, S. J. Berl, and C. A. Sackett, 2020, *Phys. Rev. Lett.* **124**(12).

Mohanty, P., 1999, *Annalen der Physik* **8**(7-9), 549.

Morizot, O., Y. Colombe, V. Lorent, H. Perrin, and B. M. Garraway, 2006, *Phys. Rev. A* **74**(2), 023617.

Moukouri, S., Y. Japha, M. Keil, T. David, D. Groswasser, M. Givon, and R. Folman, 2021, Multi-pass guided atomic sagnac interferometer for high-performance rotation sensing, eprint 2107.03446.

Moulder, S., S. Beattie, R. P. Smith, N. Tammuz, and Z. Hadzibabic, 2012, *Phys. Rev. A* **86**(1), 013629.

Mukai, T., C. Hufnagel, A. Kasper, T. Meno, A. Tsukada, K. Semba, and F. Shimizu, 2007, *Phys. Rev. Lett.* **98**(26), 260407.

Müller, D., E. A. Cornell, D. Z. Anderson, and E. R. I. Abraham, 2000, *Physical Review A* **61**(3), 033411.

Müller, D., E. A. Cornell, M. Prevedelli, P. Schwindt, A. Zozulya, and D. Z. Anderson, 2000, *Optics Letters* **25**(18), 1382 1384, ISSN 0146-9592.

Müller, H., S.-w. Chiow, Q. Long, S. Herrmann, and S. Chu, 2008, *Phys. Rev. Lett.* **100**(18), 180405.

Müller, T., B. Zhang, R. Fermani, K. Chan, M. Lim, and R. Dumke, 2010a, *Physical Review A* **81**(5), 053624.

Müller, T., B. Zhang, R. Fermani, K. Chan, Z. Wang, C. Zhang, M. Lim, and R. Dumke, 2010b, *New Journal of Physics* **12**(4), 043016.

Müllers, A., B. Santra, C. Baals, J. Jiang, J. Benary, R. Labouvie, D. A. Zezyulin, V. V. Konotop, and H. Ott, 2018, *Science Advances* **4**(8), eaat6539.

Muntinga, H., H. Ahlers, M. Krutzik, A. Wenzlawski, S. Arnold, D. Becker, K. Bongs, H. Dittus, H. Duncker, N. Gaaloul, C. Gherasim, E. Giese, et al., 2013, *Phys. Rev. Lett.* **110**, 093602.

Murmann, S., A. Bergschneider, V. M. Klinkhamer, G. Zürn, T. Lompe, and S. Jochim, 2015, *Phys. Rev. Lett.* **114**, 080402.

Murray, N., M. Krygier, M. Edwards, K. C. Wright, G. K. Campbell, and C. W. Clark, 2013, *Phys. Rev. A* **88**, 053615.

Naber, J., S. Machluf, L. Torralbo-Campo, M. Soudijn, N. Van Druten, H. V. L. Van Den Heuvell, and R. Spreeuw, 2016, *Journal of Physics B: Atomic, Molecular and Optical Physics* **49**(9), 094005.

Naldesi, P., J. P. Gomez, V. Dunjko, H. Perrin, M. Olshanii, L. Amico, and A. Minguzzi, 2019a, arXiv preprint arXiv:1901.09398 , arXiv:1901.09398.

Naldesi, P., J. P. Gomez, B. Malomed, M. Olshanii, A. Minguzzi, and L. Amico, 2019b, *Phys. Rev. Lett.* **122**, 053001.

Navez, P., S. Pandey, H. Mas, K. Poulios, T. Fernholz, and W. von Klitzing, 2016, *New Journal of Physics* **18**(7), 075014.

Nazarov, Y. V., and Y. M. Blanter, 2009, *Quantum Transport:*

Introduction to Nanoscience (Cambridge University Press). Nicolau, E., J. Mompart, B. Juliá-Díaz, and V. Ahufinger, 2020, Phys. Rev. A **102**, 023331.

Nietner, C., G. Schaller, and T. Brandes, 2014, Phys. Rev. A **89**, 013605.

Nirrengarten, T., A. Qarry, C. Roux, A. Emmert, G. Nogues, M. Brune, J.-M. Raimond, and S. Haroche, 2006, Phys. Rev. Lett. **97**(20), 200405.

Nitzan, A., and M. A. Ratner, 2003, Science **300**(5624), 1384.

Nogrette, F., H. Labuhn, S. Ravets, D. Barredo, L. Béguin, A. Vernier, T. Lahaye, and A. Browaeys, 2014, Phys. Rev. X **4**, 021034.

Nunnenkamp, A., A. M. Rey, and K. Burnett, 2008, Physical Review A **77**(2), 023622.

Nunnenkamp, A., A. M. Rey, and K. Burnett, 2011, Phys. Rev. A **84**(5), 053604.

Oelkers, N., and J. Links, 2007, Phys. Rev. B **75**, 115119.

Olariu, S., and I. I. Popescu, 1985, Rev. Mod. Phys. **57**, 339.

Olson, S. E., M. L. Terraciano, M. Bashkansky, and F. K. Fatemi, 2007, Physical Review A (Atomic, Molecular, and Optical Physics) **76**(6), 061404.

Onofrio, R., D. S. Durfee, C. Raman, M. Kohl, C. E. Kuklewicz, and W. Ketterle, 2000, Physical Review Letters **84**(5), 810.

Ozawa, T., and G. Baym, 2010, Physical Review A **82**(6), 063615.

Ozawa, T., and H. M. Price, 2019, Nature Reviews Physics **1**(5), 349.

Packard, R. E., 1998, Rev. Mod. Phys. **70**, 641.

Pagano, G., M. Mancini, G. Cappellini, L. Livi, C. Sias, J. Catani, M. Inguscio, and L. Fallami, 2015, Phys. Rev. Lett. **115**(26), 265301.

Pandey, S., H. Mas, G. Drougakis, P. Thekkepatt, V. Bolpasi, G. Vasilakis, K. Poullos, and W. von Klitzing, 2019, Nature **570**(7760), 1.

Pandey, S., H. Mas, G. Vasilakis, and W. von Klitzing, 2021, Physical Review Letters **126**(17).

Papoular, D. J., L. P. Pitaevskii, and S. Stringari, 2014, Phys. Rev. Lett. **113**, 170601.

Papoular, D. J., L. P. Pitaevskii, and S. Stringari, 2016, Phys. Rev. A **94**, 023622.

Pecci, G., P. Naldesi, A. Minguzzi, and L. Amico, 2020, arXiv preprint arXiv:2010.03552 .

Pecci, G., P. Naldesi, A. Minguzzi, and L. Amico, 2021, arXiv preprint arXiv:2105.XXXX .

Peierls, R., 1933, Zeitschrift für Physik **80**(11-12), 763.

Pelegrí, G., 2018, **20**(10), 103001.

Pepino, R., J. Cooper, D. Anderson, and M. Holland, 2009, Phys. Rev. Lett. **103**(14), 140405.

Pepino, R. A., 2021, Entropy **23**(5), 534.

Perrin, H., and B. M. Garraway, 2017, Advances In Atomic, Molecular, and Optical Physics .

Pershoguba, S. S., and L. I. Glazman, 2019, Phys. Rev. B **99**, 134514.

Peters, A., K. Y. Chung, and S. Chu, 2001, Metrologia **38**(1), 25.

Petrich, W., M. H. Anderson, J. R. Ensher, and E. A. Cornell, 1995, Physical Review Letters **74**(17), 3352.

Petrosyan, D., K. Mølmer, J. Fortágh, and M. Saffman, 2019, New Journal of Physics **21**(7), 073033.

Pezzè, L., A. Smerzi, M. K. Oberthaler, R. Schmied, and P. Treutlein, 2018, Rev. Mod. Phys. **90**, 035005.

Piazza, F., L. A. Collins, and A. Smerzi, 2009, Phys. Rev. A **80**(2), 021601(R).

Pigneur, M., T. Berrada, M. Bonneau, T. Schumm, E. Demler, and J. Schmiedmayer, 2018, Phys. Rev. Lett. **120**, 173601.

Polo, J., and V. Ahufinger, 2013, Physical Review A **88**(5), 053628.

Polo, J., V. Ahufinger, F. W. Hekking, and A. Minguzzi, 2018, Phys. Rev. Lett. **121**(9), 090404.

Polo, J., A. Benseñy, T. Busch, V. Ahufinger, and J. Mompart, 2016, New J. Phys. **18**(1), 015010.

Polo, J., R. Dubessy, P. Pedri, H. Perrin, and A. Minguzzi, 2019, Phys. Rev. Lett. **123**, 195301.

Polo, J., P. Naldesi, A. Minguzzi, and L. Amico, 2020, arXiv preprint arXiv:2012.06269 .

Price, H. M., T. Ozawa, and N. Goldman, 2017, Phys. Rev. A **95**, 023607.

Pritchard, D. E., 1983, Physical Review Letters **51**(15), 1336.

Pritchard, J. D., A. N. Dinkelaker, A. S. Arnold, P. F. Griffin, and E. Riis, 2012, New Journal of Physics **14**(10), 103047.

Pyykkönen, V. A. J., S. Peotta, P. Fabritius, J. Mohan, T. Esslinger, and P. Törmä, 2021, Phys. Rev. B **103**, 144519.

Qi, L., Z. Hu, T. Valenzuela, Y. Zhang, Y. Zhai, W. Quan, N. Waltham, and J. Fang, 2017, Applied Physics Letters **110**(15), 153502.

Ramanathan, A., K. C. Wright, S. R. Muniz, M. Zelan, W. T. Hill, C. J. Lobb, K. Helmerson, W. D. Phillips, and G. K. Campbell, 2011, Phys. Rev. Lett. **106**(13), 130401.

Rapp, A., G. Zaránd, C. Honerkamp, and W. Hofstetter, 2007, Phys. Rev. Lett. **98**(16), 160405.

Reichel, J., W. Hänsel, and T. W. Hänsch, 1999, Physical Review Letters **83**(17), 3398, URL <https://doi.org/10.1103/physrevlett.83.3398>.

Renn, M. J., E. A. Donley, E. A. Cornell, C. E. Wieman, and D. Z. Anderson, 1996, Physical Review A **53**(2), R648.

Rhodes, D. P., G. P. T. Lancaster, J. Livesey, D. McGloin, J. Arlt, and K. Dholakia, 2002, Optics Communications **214**(1-6), 247.

Riedel, E. K., and F. von Oppen, 1993, Physical Review B **47**(23), 15449.

Rieger, T., T. Junglen, S. A. Rangwala, P. W. Pinkse, and G. Rempe, 2005, Phys. Rev. Lett. **95**(17), 173002.

Rincón, J., A. Aligia, and K. Hallberg, 2009, Phys. Rev. B **79**(3), 035112.

Rincón, J., K. Hallberg, and A. Aligia, 2008, Phys. Rev. B **78**(12), 125115.

Roscilde, T., M. F. Faulkner, S. T. Bramwell, and P. C. W. Holdsworth, 2016, New J. Phys. **18**(7), 075003.

Rubinsztein-Dunlop, H., A. Forbes, M. V. Berry, M. R. Dennis, D. L. Andrews, M. Mansuripur, C. Denz, C. Alpmann, P. Banzer, T. Bauer, E. Karimi, L. Marrucci, *et al.*, 2016, Journal of Optics **19**(1), 013001.

Ruostekoski, J., and D. F. Walls, 1998, Phys. Rev. A **58**, R50.

Ryu, C., P. Blackburn, A. Blinova, and M. Boshier, 2013, Phys. Rev. Lett. **111**(20), 205301.

Ryu, C., and M. G. Boshier, 2015, New Journal of Physics **17**(9), 092002.

Ryu, C., K. C. Henderson, and M. G. Boshier, 2014, New Journal of Physics **16**(1), 013046.

Ryu, C., E. C. Samson, and M. G. Boshier, 2020, Nature Communications **11**(1), 3338.

Safaei, S., B. Grémaud, R. Dumke, L.-C. Kwek, L. Amico, and C. Miniatura, 2018, Physical Review A **97**(4), 042306.

Saffman, M., T. G. Walker, and K. Mølmer, 2010, Reviews of Modern Physics **82**(3), 2313.

Salerno, G., H. M. Price, M. Lebrat, S. Häusler, T. Esslinger, L. Corman, J.-P. Brantut, and N. Goldman, 2019, Phys. Rev. X **9**, 041001.

Salim, E. A., S. C. Caliga, J. B. Pfeiffer, and D. Z. Anderson, 2013, Applied Physics Letters **102**(8), 084104.

Saminadayar, L., C. Bauerle, and D. Mailly, 2004, Enc. Nanosci. Nanotech **4**, 267.

Sanvitto, D., F. Marchetti, M. Szymańska, G. Tosi, M. Baudisch, F. P. Laussy, D. Krizhanovskii, M. Skolnick, L. Marzocchi, A. Lemaitre, *et al.*, 2010, Nature Physics **6**(7), 527.

Sauer, J. A., M. D. Barrett, and M. S. Chapman, 2001, Phys. Rev. Lett. **87**(27), 270401.

Schenke, C., A. Minguzzi, and F. W. J. Hekking, 2011, Phys. Rev. A **84**, 053636.

Schmiedmayer, J., 1995a, Physical Review A **52**(1), R13.

Schmiedmayer, J., 1995b, Applied Physics B **60**(2), 169.

Schmiedmayer, J., and A. Scrinzi, 1996a, Quantum and Semiclassical Optics: Journal of the European Optical Society Part B **8**(3), 693.

Schmiedmayer, J., and A. Scrinzi, 1996b, Physical Review A **54**(4), R2525.

Schnelle, S. K., E. D. Van Ooijen, M. J. Davis, N. R. Heckenberg, and H. Rubinsztein-Dunlop, 2008, Optics Express **16**(3), 1405.

Schumm, T., S. Hofferberth, L. M. Andersson, S. Wildermuth, S. Groth, I. Bar-Joseph, J. Schmiedmayer, and P. Kruger, 2005, Nature Physics **1**(1), 57.

Schweigler, T., M. Gluza, M. Tajik, S. Sotiriadis, F. Cataldini, S.-C. Ji, F. S. Møller, J. Sabino, B. Rauer, J. Eisert, and J. Schmiedmayer, 2021, Nature Physics **17**(5), 559.

Seaman, B., M. Krämer, D. Anderson, and M. Holland, 2007, Phys. Rev. A **75**(2), 023615.

Sekera, T., C. Bruder, and W. Belzig, 2016, Phys. Rev. A **94**, 033618.

Shmakov, P., A. Dmitriev, and V. Y. Kachorovskii, 2013, Phys. Rev. B **87**(23), 235417.

Shuman, E. S., J. F. Barry, and D. DeMille, 2010, Nature **467**(7317), 820.

Simpson, D., D. Gangardt, I. Lerner, and P. Krüger, 2014, Physical review letters **112**(10), 100601.

Sinclair, C. D. J., E. A. Curtis, I. L. Garcia, J. A. Retter, B. V. Hall, S. Eriksson, B. E. Sauer, and E. A. Hinds, 2005, Physical Review A **72**, 031603.

Singh, V. P., N. Luick, L. Sobirey, and L. Mathey, 2020, Phys. Rev. Research **2**, 033298.

Sinuoco-León, G. A., K. A. Burrows, A. S. Arnold, and B. M. Garraway, 2014, Nature Communications **5**(1), URL <https://doi.org/10.1038/ncomms6289>.

Smerzi, A., S. Fantoni, S. Giovanazzi, and S. Shenoy, 1997, Phys. Rev. Lett. **79**(25), 4950.

Solenov, D., and D. Mozyrsky, 2010, Physical Review A **82**(6), 061601.

Sommer, A., M. Ku, G. Roati, and M. W. Zwierlein, 2011, Nature **472**(7342), 201.

Spagnolli, G., G. Semeghini, L. Masi, G. Ferioli, A. Trenkwalder, S. Coop, M. Landini, L. Pezzè, G. Modugno, M. Inguscio, A. Smerzi, and M. Fattori, 2017, Phys. Rev. Lett. **118**, 230403.

Spehner, D., L. Morales-Molina, and S. A. Reyes, 2021, New Journal of Physics .

Stadler, D., S. Krinner, J. Meineke, J.-P. Brantut, and T. Esslinger, 2012, Nature **491**(7426), 736.

Stevenson, R., M. R. Hush, T. Bishop, I. Lesanovsky, and T. Fernholz, 2015, Physical Review Letters **115**, 163001.

Stickney, J. A., D. Z. Anderson, and A. A. Zozulya, 2007, Physical Review A **75**(1), 013608.

Stockton, J., K. Takase, and M. Kasevich, 2011, Phys. Rev. Lett. **107**(13), 133001.

Sugarbaker, A., S. M. Dickerson, J. M. Hogan, D. M. Johnson, and M. A. Kasevich, ????

Sun, K., K. Padavić, F. Yang, S. Vishveshwara, and C. Lantert, 2018, Physical Review A **98**(1).

Surace, F. M., and A. Lerose, 2021, New Journal of Physics **23**(6), 062001.

Sutherland, B., 1968, Phys. Rev. Lett. **20**(3), 98.

Sutherland, B., 1975, Phys. Rev. B **12**, 3795.

Tajik, M., B. Rauer, T. Schweigler, F. Cataldini, J. Sabino, F. S. Møller, S.-C. Ji, I. E. Mazets, and J. Schmiedmayer, 2019, Optics Express **27**(23), 33474, URL <https://doi.org/10.1364/OE.27.033474>.

Thouless, D., 1983, Phys. Rev. B **27**(10), 6083.

Thouless, D. J., M. Kohmoto, M. P. Nightingale, and M. den Nijs, 1982, Phys. Rev. Lett. **49**(6), 405.

Tinkham, M., 2012, *Introduction to superconductivity* (Courier Dover Publications).

Tokuno, A., M. Oshikawa, and E. Demler, 2008, Phys. Rev. Lett. **100**(14), 140402.

Tollett, J. J., C. C. Bradley, C. A. Sackett, and R. G. Hulet, 1995, Phys. Rev. A **51**, R22.

Tononi, A., F. Toigo, S. Wimberger, A. Cappellaro, and L. Salasnich, 2020, New Journal of Physics **22**(7), 073020.

Tosto, F., P. Baw Swe, N. T. Nguyen, C. Hufnagel, M. Martínez Valado, L. Prigozhin, V. Sokolovsky, and R. Dumke, 2019, Applied Physics Letters **114**(22), 222601.

Trebbia, J.-B., C. L. Garrido Alzar, R. Cornelussen, C. I. Westbrook, and I. Bouchoule, 2007, Phys. Rev. Lett. **98**, 263201.

Trenkwalder, A., G. Spagnolli, G. Semeghini, S. Coop, M. Landini, P. Castilho, L. Pezzè, G. Modugno, M. Inguscio, A. Smerzi, and M. Fattori, 2016, Nature Physics **12**(9), 826.

Truscott, A. G., K. E. Strecker, W. I. McAlexander, G. B. Partridge, and R. G. Hulet, 2001, Science **291**(5513), 2570.

Turpin, A., J. Polo, Y. V. Loiko, J. Kübler, F. Schmaltz, T. K. Kalkandjiev, V. Ahufinger, G. Birk, and J. Mompart, 2015, Optics Express **23**(2), 1638.

Uchino, S., 2020, Phys. Rev. Research **2**, 023340.

Uchino, S., and J.-P. Brantut, 2020, Phys. Rev. Research **2**, 023284.

Uchino, S., and M. Ueda, 2017, Phys. Rev. Lett. **118**, 105303.

Uchino, S., M. Ueda, and J.-P. Brantut, 2018, Phys. Rev. A **98**, 063619.

Vaidman, L., 2012, Physical Review A **86**(4), URL <https://doi.org/10.1103/physreva.86.040101>.

Valtolina, G., A. Burchianti, A. Amico, E. Neri, K. Xhani, J. A. Seman, A. Trombettoni, A. Smerzi, M. Zaccanti, M. Inguscio, and G. Roati, 2015, Science **350**(6267), 1505.

Valtolina, G., F. Scazza, A. Amico, A. Burchianti, A. Recati, T. Enss, M. Inguscio, M. Zaccanti, and G. Roati, 2017, Nat. Phys. **13**(7), 704.

Verdú, J., H. Zoubi, C. Koller, J. Majer, H. Ritsch, and J. Schmiedmayer, 2009, Phys. Rev. Lett. **103**(4), 043603.

Victorin, N., T. Haug, L.-C. Kwek, L. Amico, and A. Minguzzi, 2019, Physical Review A **99**(3), 033616.

Victorin, N., F. Hekking, and A. Minguzzi, 2018, Phys. Rev. A **98**, 053626.

Waintal, X., G. Fleury, K. Kazymyrenko, M. Houzet, P. Schmitteckert, and D. Weinmann, 2008, Phys. Rev. Lett.

101(10), 106804.

Wang, Y., S. Subhankar, P. Bienias, M. Lacki, T.-C. Tsui, M. A. Baranov, A. V. Gorshkov, P. Zoller, J. V. Porto, and S. L. Rolston, 2018, Physical Review Letters **120**(8), 083601, ISSN 0031-9007.

Wang, Y.-H., A. Kumar, F. Jendrzejewski, R. M. Wilson, M. Edwards, S. Eckel, G. K. Campbell, and C. W. Clark, 2015, New Journal of Physics **17**, 125012.

Wang, Y.-J., D. Z. Anderson, V. M. Bright, E. A. Cornell, Q. Diot, T. Kishimoto, M. Prentiss, R. A. Saravanan, S. R. Segal, and S. Wu, 2005, Physical Review Letters **94**(9), 090405.

Watabe, S., and Y. Kato, 2008, Phys. Rev. A **78**(6), 063611.

Webb, R. A., S. Washburn, C. Umbach, and R. Laibowitz, 1985, Phys. Rev. Lett. **54**(25), 2696.

van Wees, B. J., H. van Houten, C. W. J. Beenakker, J. G. Williamson, L. P. Kouwenhoven, D. van der Marel, and C. T. Foxon, 1988, Phys. Rev. Lett. **60**, 848.

Weiss, C., and Y. Castin, 2009, Phys. Rev. Lett. **102**(1), 010403.

Wharam, D. A., T. J. Thornton, R. Newbury, M. Pepper, H. Ahmed, J. E. F. Frost, D. G. Hasko, D. C. Peacock, D. A. Ritchie, and G. A. C. Jones, 1988, Journal of Physics C: Solid State Physics **21**(8), L209.

White, D. H., T. A. Haase, D. J. Brown, M. D. Hoogerland, M. S. Najafabadi, J. L. Helm, C. Gies, D. Schumayer, and D. A. Hutchinson, 2019, arXiv preprint arXiv:1911.04858.

Wildermuth, S., S. Hofferberth, I. Lesanovsky, S. Groth, P. Krüger, J. Schmiedmayer, and I. Bar-Joseph, 2006, Applied physics letters **88**(26), 264103.

Wright, E., J. Arlt, and K. Dholakia, 2000, Physical Review A **63**(1), 013608.

Wright, K. C., R. B. Blakestad, C. J. Lobb, W. D. Phillips, and G. K. Campbell, 2013a, Phys. Rev. Lett. **110**(2), 025302.

Wright, K. C., R. B. Blakestad, C. J. Lobb, W. D. Phillips, and G. K. Campbell, 2013b, Phys. Rev. A **88**(6), 063633.

Wu, S., E. Su, and M. Prentiss, 2007, Phys. Rev. Lett. **99**(17).

Wu, S., Y.-J. Wang, Q. Diot, and M. Prentiss, 2005, Physical Review A **71**(4), 043602.

Xhani, K., E. Neri, L. Galantucci, F. Scazza, A. Burchianti, K.-L. Lee, C. F. Barenghi, A. Trombettoni, M. Inguscio, M. Zaccanti, G. Roati, and N. P. Proukakis, 2020, Phys. Rev. Lett. **124**, 045301.

Xiang, Z.-L., S. Ashhab, J. Q. You, and F. Nori, 2013, Rev. Mod. Phys. **85**(2), 623.

Yao, J., B. Liu, M. Sun, and H. Zhai, 2018, Phys. Rev. A **98**, 041601.

You, J.-S., R. Schmidt, D. A. Ivanov, M. Knap, and E. Demler, 2019, Phys. Rev. B **99**, 214505.

Yu, D., L. C. Kwek, L. Amico, and R. Dumke, 2017a, Quantum Science and Technology **2**(3), 035005.

Yu, D., L. C. Kwek, L. Amico, and R. Dumke, 2017b, Physical Review A **95**(5), 053811.

Yu, D., L. C. Kwek, L. Amico, and R. Dumke, 2018a, Phys. Rev. A **98**, 033833.

Yu, D., A. Landra, L. C. Kwek, L. Amico, and R. Dumke, 2018b, New Journal of Physics **20**(2), 023031.

Yu, D., A. Landra, M. M. Valado, C. Hufnagel, L. C. Kwek, L. Amico, and R. Dumke, 2016a, Physical Review A **94**(6), 062301.

Yu, D., M. M. Valado, C. Hufnagel, L. C. Kwek, L. Amico, and R. Dumke, 2016b, Physical Review A **93**(4), 042329.

Yu, D., M. M. Valado, C. Hufnagel, L. C. Kwek, L. Amico, and R. Dumke, 2016c, Scientific Reports **6**, 38356.

Yu, N., and M. Fowler, 1992, Phys. Rev. B **45**, 11795.

Zabow, G., R. S. Conroy, and M. G. Prentiss, 2004, Phys. Rev. Lett. **92**(18), 180404.

Zaccanti, M., and W. Zwerger, 2019, Phys. Rev. A **100**, 063601.

Zapata, I., and F. Sols, 2009, Phys. Rev. Lett. **102**(18), 180405.

Zapata, I., F. Sols, and A. J. Leggett, 1998, Phys. Rev. A **57**, R28.

Zhang, B., M. Siercke, K. S. Chan, M. Beian, M. J. Lim, and R. Dumke, 2012, Phys. Rev. A **85**, 013404.

Zobay, O., and B. M. Garraway, 2001, Phys. Rev. Lett. **86**(7), 1195.

van Zoest, T., N. Gaaloul, Y. Singh, H. Ahlers, W. Herr, S. Seidel, W. Ertmer, E. Rasel, M. Eckart, E. Kajari, et al., 2010, Science **328**(5985), 1540.

Zöllner, S., H.-D. Meyer, and P. Schmelcher, 2008, Phys. Rev. Lett. **100**, 040401.

Zou, Y. Q., E. Le Cerf, B. Bakkali-Hassani, C. Maury, G. Chauveau, P. C. M. Castilho, R. Saint-Jalm, S. Nascimbene, J. Dalibard, and J. Beugnon, 2021, Journal of Physics B: Atomic, Molecular and Optical Physics **54**(8), 08LT01.

Zozulya, A. A., and D. Z. Anderson, 2013, Physical Review A **88**(4).

Zupancic, P., P. M. Preiss, R. Ma, A. Lukin, M. E. Tai, M. Rispoli, R. Islam, and M. Greiner, 2016, Optics Express **24**(13), 13881.

Zvyagin, A. A., and I. V. Krive, 1995, Low Temperature Physics **21**, 533.